Supplementary Material

UPF2 leads to degradation of dendritically-targeted mRNAs to regulate synaptic plasticity and cognitive function.

Michael Notaras[1], Megan Allen[1], Francesco Longo[2], Nicole Volk[1], Miklos Toth[3], Noo Li Jeon[4], Eric Klann[2], Dilek Colak[1,5,*]

[1] Center for Neurogenetics, Feil Family Brain and Mind Research Institute, Weill Cornell Medical College, Cornell University, New York City, New York, USA.
[2] Center for Neural Science, New York University, New York City, New York, USA.
[3] Department of Pharmacology, Weill Cornell Medical College, Cornell University, New York City, New York, USA.
[4] School of Mechanical and Aerospace Engineering, Seoul National University, Seoul, South Korea.
[5] Gale & Ira Drukier Institute for Children's Health, Weill Cornell Medical College, Cornell University, New York City, New York, USA.

*Correspondence: dic2009@med.cornell.edu

Figure S1.

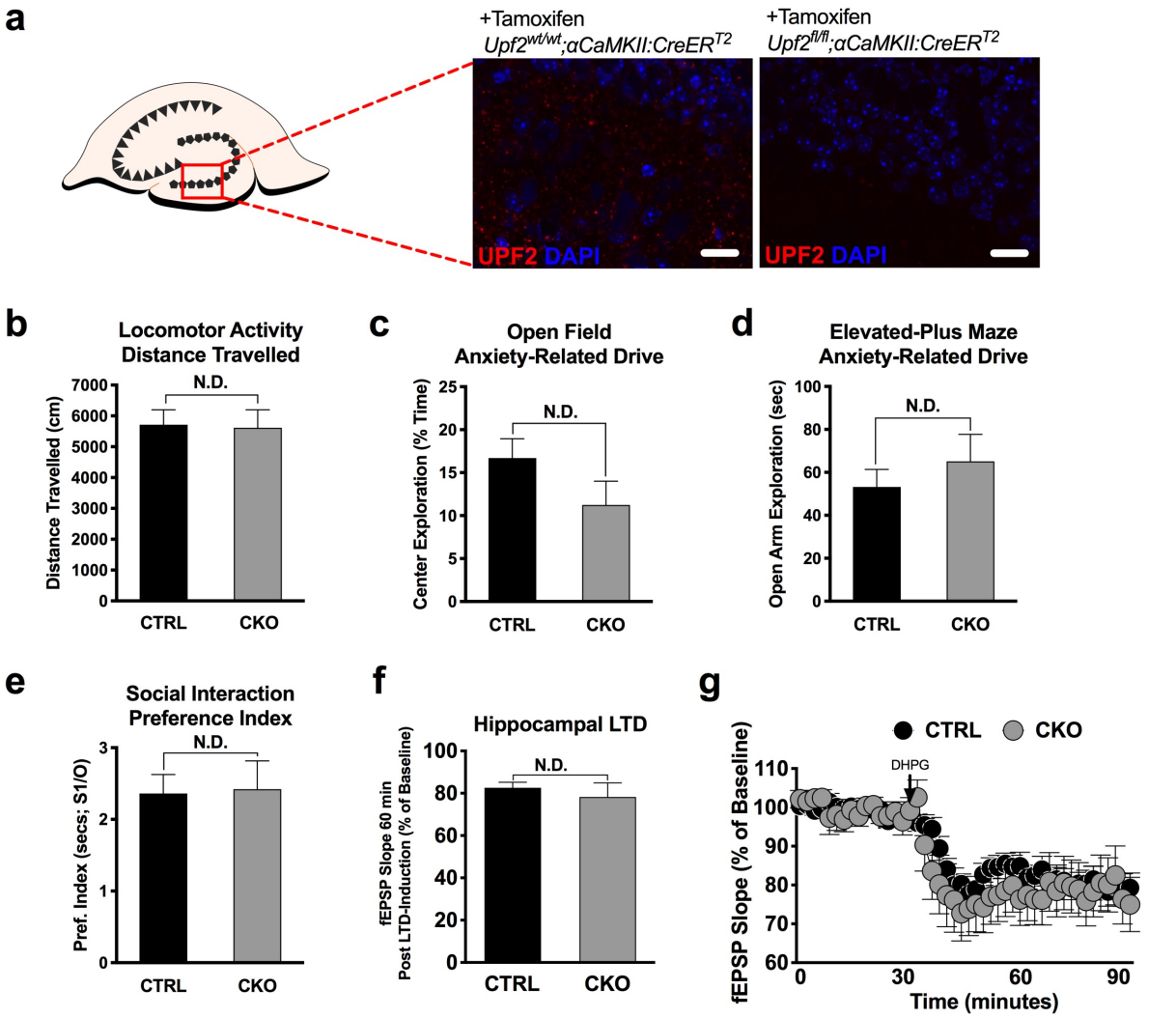
a
+Tamoxifen
Upf2wt/wt;αCaMKII:CreERT2
+Tamoxifen
Upf2fl/fl;αCaMKII:CreERT2
UPF2 DAPI
UPF2 DAPI
b
Locomotor Activity
Distance Travelled
Distance Travelled (cm)
N.D.
CTRL
CKO
c
Open Field
Anxiety-Related Drive
Center Exploration (% Time)
N.D.
CTRL
CKO
d
Elevated-Plus Maze
Anxiety-Related Drive
Open Arm Exploration (sec)
N.D.
CTRL
CKO
e
Social Interaction
Preference Index
Pref. Index (secs; S1/O)
N.D.
CTRL
CKO
f
Hippocampal LTD
fEPSP Slope 60 min
Post LTD-Induction (% of Baseline)
N.D.
CTRL
CKO
g
CTRL
CKO
DHPG
fEPSP Slope (% of Baseline)
Time (minutes)

Figure S1. UPF2 does not influence baseline locomotor activity, anxiety-related behavior, sociability, and LTD in mice.

a, To determine the potential role of NMD in hippocampus-dependent cognition in the adult brain, we disrupted NMD in postmitotic neurons using a conditional knockout mouse of *Upf2* (*Upf2*$^{fl/fl}$) [1]. To temporally control *Upf2* knockdown, we crossed *Upf2*$^{fl/fl}$ mice with a mouse line that expresses tamoxifen-inducible Cre under the α*CaMKII* promoter (α*CaMKII*::*CreER*^{T2}) [2]. Before assessing synaptic plasticity and learning and memory (Figure 1) in *Upf2*$^{fl/fl}$;α*CaMKII*:*CreER*^{T2} (CKO) and *Upf2*$^{wt/wt}$;α*CaMKII*:*CreER*^{T2} (CTRL) mice, we confirmed that conditional deletion of *Upf2* gene (using 200 mg/kg Tamoxifen, for 5 doses) led to the successful loss of UPF2 protein in the hippocampus.

b-d, To determine whether UPF2 induces hyperactivity, mice were subjected to a 2 hr locomotor hyperactivity assay in photocells. During this 2 hr trial, the distance that mice travelled in cm was analyzed. Greater distances travelled are used as an indicator of locomotor hyperactivity, which may confound behavioral testing on other maze tasks. Similarly, this assay can also assess hypoactivity induced by genetic alterations, which may also influence task performance.

b, In our assessment of baseline locomotor activity, there were no genotype differences between CTRL (n=25) and CKO (n=22) mice. This indicates that loss of UPF2 does not result in acquired hyper- or hypoactivity.

c, A 10 min open field assay was also conducted in locomotor photocells as an additional control assay, with less time spent exploring the center field of photocells being interpreted as an anxiety-like phenotype. Consistent with the outcome of the locomotor activity assay, no evidence of anxiety-like behavior between CTRL (n=25) and CKO (n=22) mice emerged on this test, suggesting that NMD does not modify anxiety-related behavior.

d, The elevated-plus maze was used as a control assay to ensure that NMD did not modify anxiety-related exploratory drive, which may compound measurements of learning and memory. Briefly, mice were subjected to a 10 min test session, with time spent exploring the open arms being used as an index of anxiety-like behavior. No genotype differences emerged between CTRL (n=25) and CKO (n=22) mice on this test.

e, Alterations in both spine density and GLUR1 levels are linked to deficits in sociability [3, 4]. In addition, defects in the NMD machinery are linked to numerous neurodevelopmental diseases associated with alterations in normal social behavior [5-10]. To determine whether NMD is required for sociability, we used the three-chamber social interaction task and measured sociability in CTRL and CKO mice. Mice were habituated to the empty three-chamber apparatus for 10 min before being exposed to a stranger mouse placed inside a cup in one chamber and an empty cup in the opposite chamber for an additional 5 min. A preference index was derived from time spent sniffing or interacting with the cup containing the stranger mouse divided by time spent interacting with the empty cup, with higher preference indexes representing more social behavior. No significant differences in preference index emerged between CTRL (n=24) and CKO (n=19) mice on the three-chamber social interaction assay.

f-g, NMD regulates spine density and L-LTP in hippocampus (Figure 1j-m). We also assayed LTD in *Upf2* CKO. Because of age-related decline in LTD, we induced Cre at 3 weeks of age and hippocampal slices were acquired from 6 week-old CTRL and CKO mice (see Methods). LTD was induced by acute application of 100 μM DHPG for 10 min to hippocampal slices. fEPSPs were collected for 60 min post-LTD induction. Compared to CTRL mice (n=14 slices from 7 mice), CKO mice (n=10 slices from 5 mice) did not show significantly different slope values post-DHPG application indicating that LTD is unaltered in the absence of NMD in hippocampus.
Data are represented as mean ± SEM; N.D. represents “No Difference”. Scale bar: 15 μm.

Figure S2

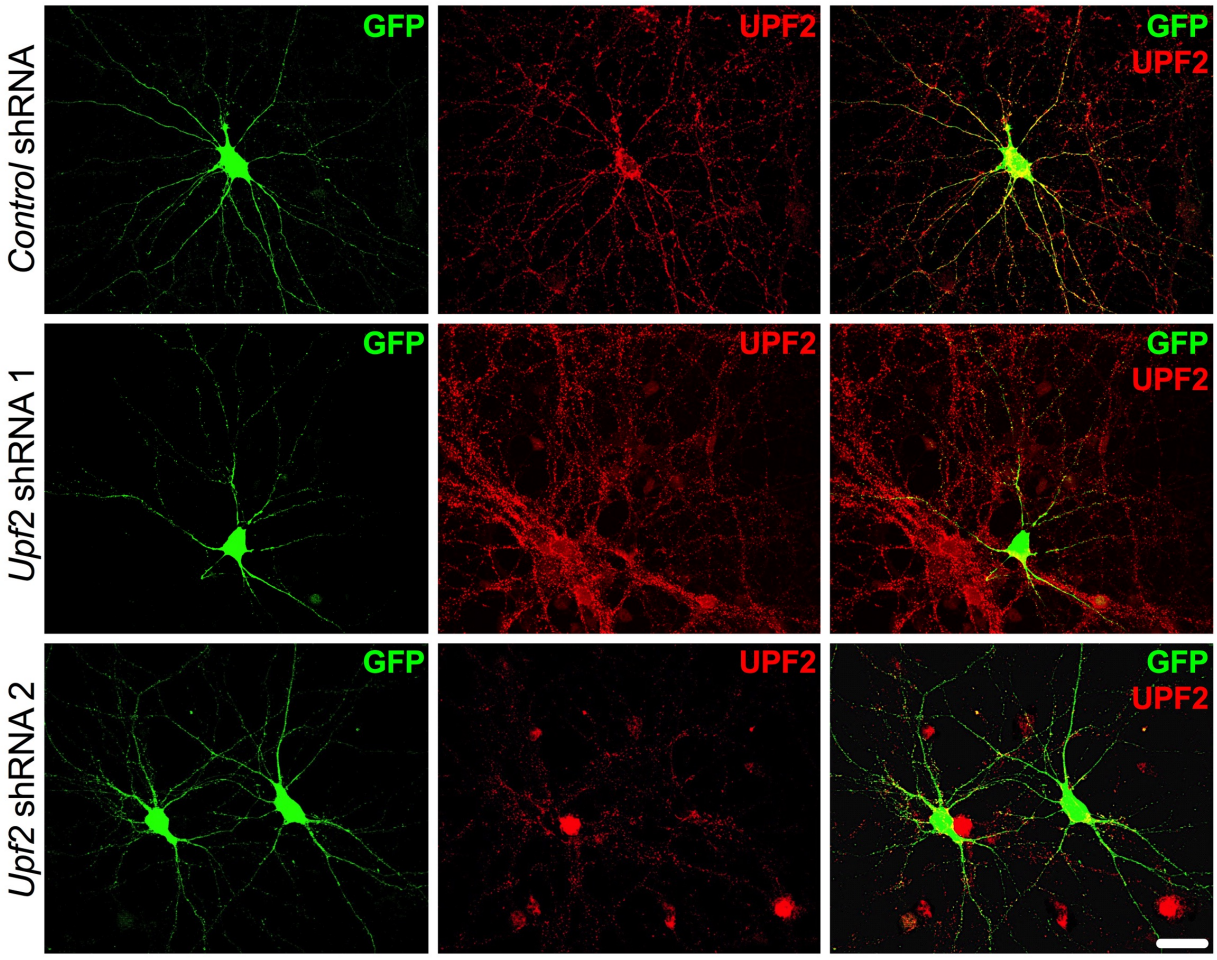
Control shRNA
Upf2 shRNA 1
Upf2 shRNA 2
GFP
UPF2
GFP
UPF2

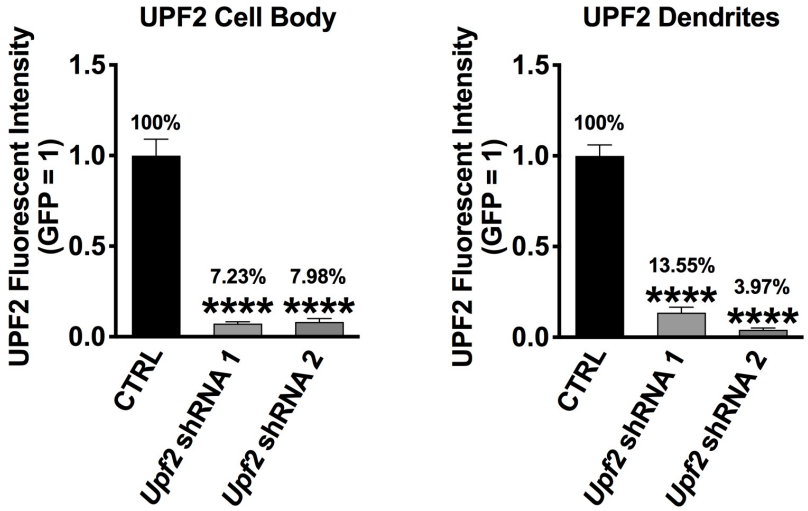
UPF2 Cell Body
UPF2 Fluorescent Intensity (GFP = 1)
1.5
1.0
0.5
0.0
100%
7.23%
7.98%
****
****
CTRL
Upf2 shRNA 1
Upf2 shRNA 2
UPF2 Dendrites
UPF2 Fluorescent Intensity (GFP = 1)
1.5
1.0
0.5
0.0
100%
13.55%
3.97%
****
****
CTRL
Upf2 shRNA 1
Upf2 shRNA 2

Figure S2. Knockdown of *Upf2* in mouse hippocampal neurons by *Upf2*-shRNA:GFP lentivirus.
To disrupt NMD, we targeted the *Upf2* mRNA using *Upf2*-shRNA:GFP lentivirus. Canonical NMD involves the interaction of UPF1, UPF2 and UPF3 proteins. While UPF1 function is not restricted to the NMD pathway [11], *Upf2* has been successfully targeted to disrupt NMD in several studies [1, 12, 13]. We infected E16 hippocampal neurons at DIV7 with *control*- or two independent *Upf2*-shRNA viruses. To assess the disruption of UPF2 protein, we fixed the cells at DIV14 and performed immunohistochemistry for UPF2. Application of both *Upf2*-shRNA viruses resulted in a robust depletion of UPF2 within infected neurons and their dendrites, while UPF2 expression remained intact in scrambled *control*-shRNA cultures and non-infected neurons in *Upf2*-shRNA cultures (UPF2+, GFP- cells in *Upf2*-shRNA 2 panel). This control experiment with two separate viruses targeting non-overlapping UPF2 sequences exemplifies specific knockdown of *Upf2* between constructs and across our studies. Thus, this control experimentation ensures that the phenotypes that arise from this knockdown are unlikely to originate from off-target effects. Scale bar: 30 μm.

Figure S3.

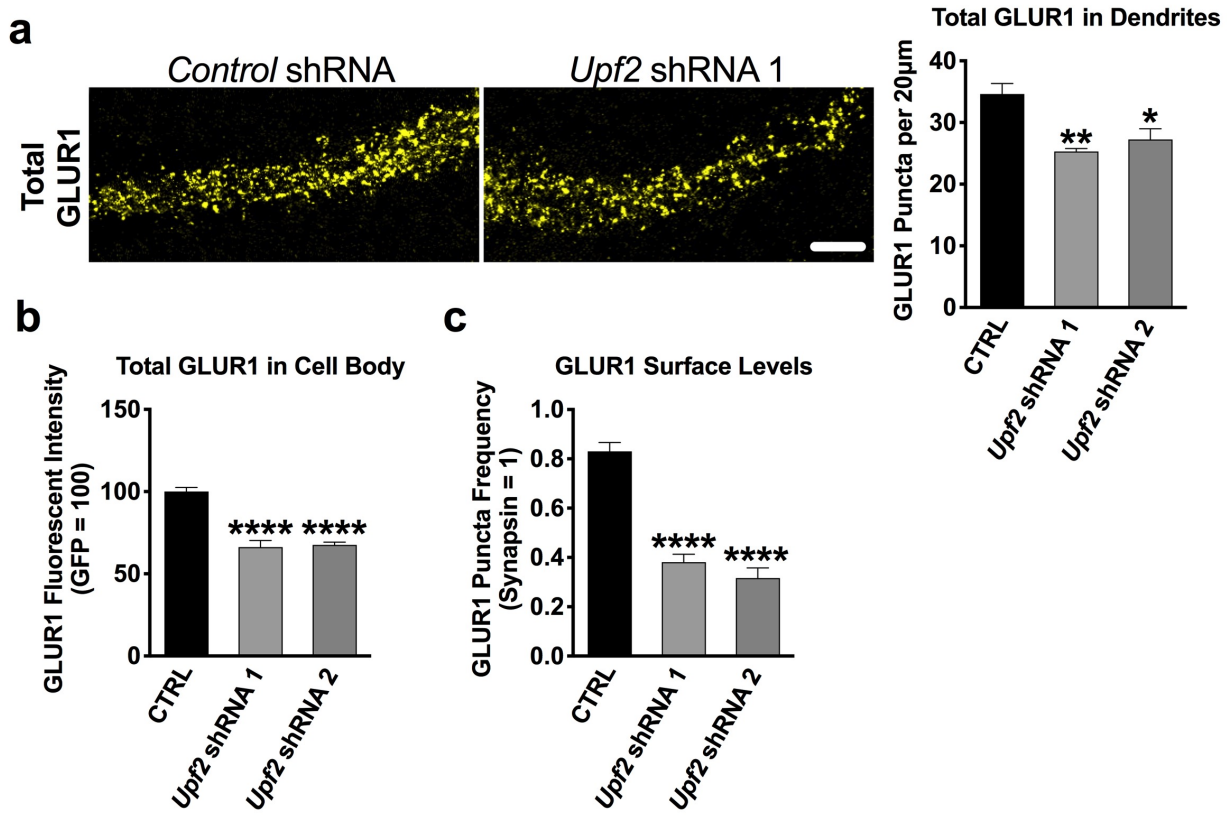
a
Control shRNA
Upf2 shRNA 1
Total GLUR1
Total GLUR1 in Dendrites
GLUR1 Puncta per 20µm
40
30
20
10
0
**
*
CTRL
Upf2 shRNA 1
Upf2 shRNA 2
b
Total GLUR1 in Cell Body
GLUR1 Fluorescent Intensity (GFP = 100)
150
100
50
0
**** ****
CTRL
Upf2 shRNA 1
Upf2 shRNA 2
c
GLUR1 Surface Levels
GLUR1 Puncta Frequency (Synapsin = 1)
1.0
0.8
0.6
0.4
0.2
0.0
**** ****
CTRL
Upf2 shRNA 1
Upf2 shRNA 2

Figure S3. Total and surface levels of GLUR1 protein are decreased upon knockdown of *Upf2*.

Loss of *Upf2* led to a decrease in GLUR1 levels *in vivo* (Figure 1m). To explore this phenotype *in vitro,* we infected hippocampal neurons with the 2 independent *Upf2*-shRNA:GFP lentivirus vectors validated in Figure S2 to interrupt endogenous NMD activity. Hippocampal neurons were infected at 7 days *in vitro* (DIV7) and GLUR1 expression was examined on DIV21. We quantified total GLUR1 signal using an anti-C-terminus-GLUR1 antibody in fixed and permeabilized cells.

a, UPF2-deficient dendrites had significantly lower GLUR1 density compared to control dendrites (n=3 biological replicates per *control*-shRNA [10 neurons, 23 dendrites] and per *Upf2*-shRNA [11 neurons, 25 dendrites]; representative image reflects *Upf2*-shRNA 1, and *Upf2*-shRNA refers to the *Upf2*-shRNA 1 in the following text). This suggests that while NMD does not alter *GluR1* transcription or mRNA degradation (Figure 2d), there is either an increase in GLUR1 receptor degradation or a decrease in GLUR1 synthesis.

b, Total GLUR1 levels were also significantly decreased in the cell bodies of UPF2-deficient neurons. We measured total fluorescence signal by measuring the integrated density in a defined region using ImageJ. Knockdown of *Upf2* led to a decrease in total GLUR1 levels in cell bodies (n=3 biological replicates per *control*-shRNA [15 neurons] and per *Upf2*-shRNA [13 neurons]).

c, Surface GLUR1 expression was also quantified (see Methods) in cultures infected with both of our validated *Upf2*-shRNA:GFP lentivirus vectors. Similar to total GLUR1 levels in dendrites, surface levels of GLUR1 were also decreased in UPF2-deficient dendrites (n=3 biological replicates per *control*-shRNA [15 neurons] and per *Upf2*-shRNA [13 neurons]). Increased local internalization and decreased local synthesis of GLUR1 are likely to contribute to this phenotype (see Figure 3).

Data are represented as mean ± SEM; $^{**}p < 0.01$, and $^{***}p < 0.001$. Scale bar: 20 μm.

Figure S4.

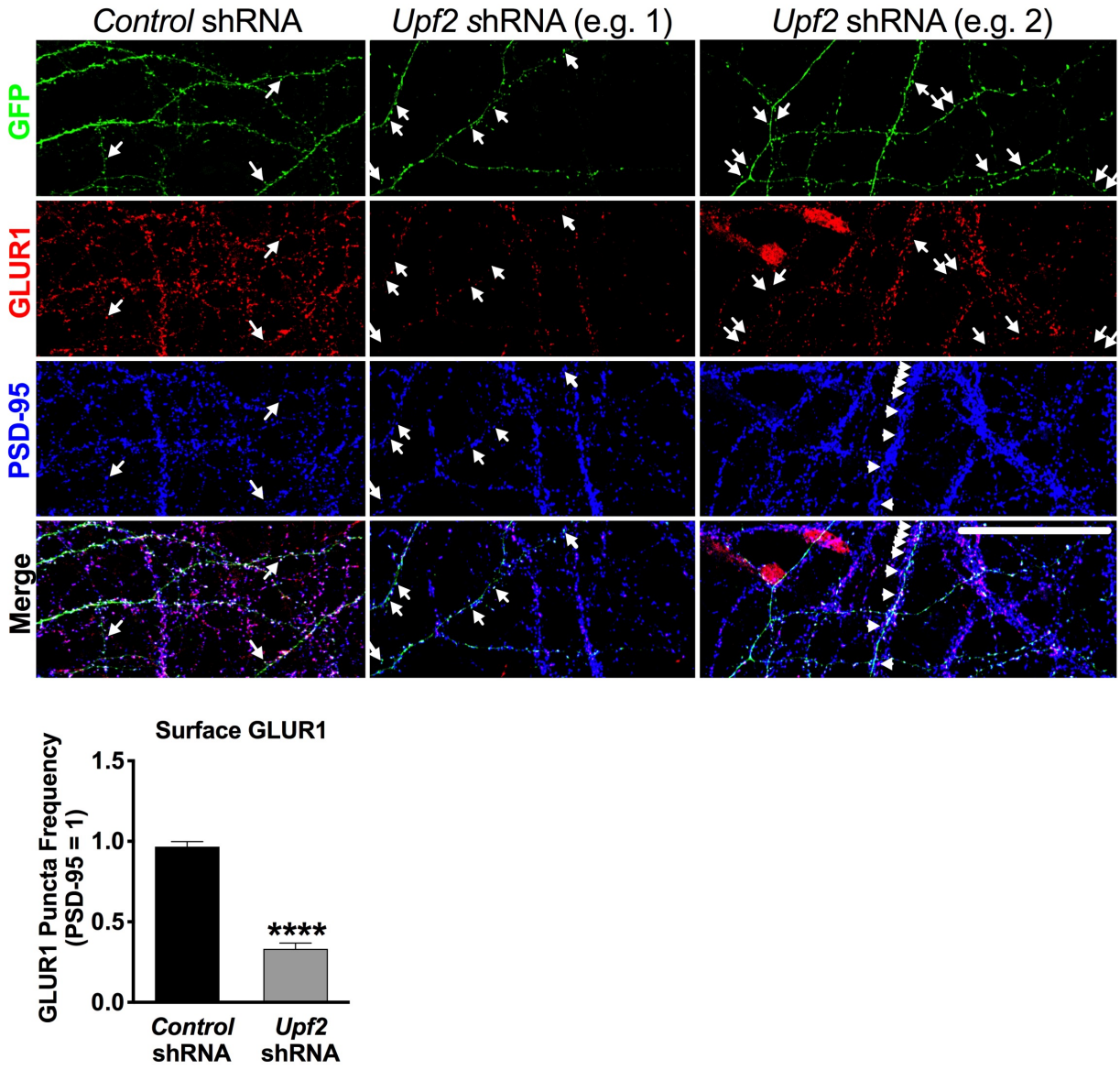
Control shRNA
Upf2 shRNA (e.g. 1)
Upf2 shRNA (e.g. 2)
GFP
GLUR1
PSD-95
Merge
Surface GLUR1
GLUR1 Puncta Frequency (PSD-95 = 1)
1.5
1.0
0.5
0.0
****
Control shRNA
Upf2 shRNA

Figure S4. Decrease in GLUR1 surface levels in UPF2-deficient dendrites was also recapitulated when the synaptic marker PSD-95, in addition to SYN1, was used for quantifications.

In Figure 2, we show that knockdown of *Upf2* in hippocampal neurons led to a robust depletion of surface GLUR1 levels without altering the mRNA transcription of this receptor. For these quantifications, we used Synapsin (SYN1) as a normalization marker as this is consistent with prior work (see Methods). To address whether this GLUR1 phenotype is recapitulated when another synaptic marker is used for normalization, we repeated this experiment using the postsynaptic marker PSD-95. Similar to the SYN1 quantifications, the disruption of UPF2 in hippocampal neurons resulted in a significant depletion of surface GLUR1 levels when synapses were identified and normalized against PSD-95 expression (n=3 biological replicates per group; 11 dendrites from 7 neurons for *control*-shRNA cultures, and 12 dendrites from 8 neurons for *Upf2*-shRNA cultures). Arrows show examples of GFP and GLUR1 colocalization in spines. Two panels of *Upf2*-shRNA dendrites are presented to exemplify contrasting aspects of GLUR1 expression. Arrows depict the loss of surface GLUR1 in spines of *Upf2*-shRNA infected hippocampal neurons relative to control cultures. Arrowheads in the merged panel of *Upf2*-shRNA example 2 depict a non-infected dendrite segment with intact GLUR1 expression that is overlapping an infected dendrite that exhibits reduced GLUR1 colocalization in isolated GFP+ spines. These data replicate the depletion of GLUR1 surface levels in UPF2-deficient dendrites presented in Figure 2, and provide confirmation that SYN1 produced concordant data to PSD-95 when used to evaluate surface GLUR1 levels.

Data are represented as mean ± Standard Error of the Mean (SEM); ****$p < 0.0001$. Scale bar: 30 μm.

Figure S5.

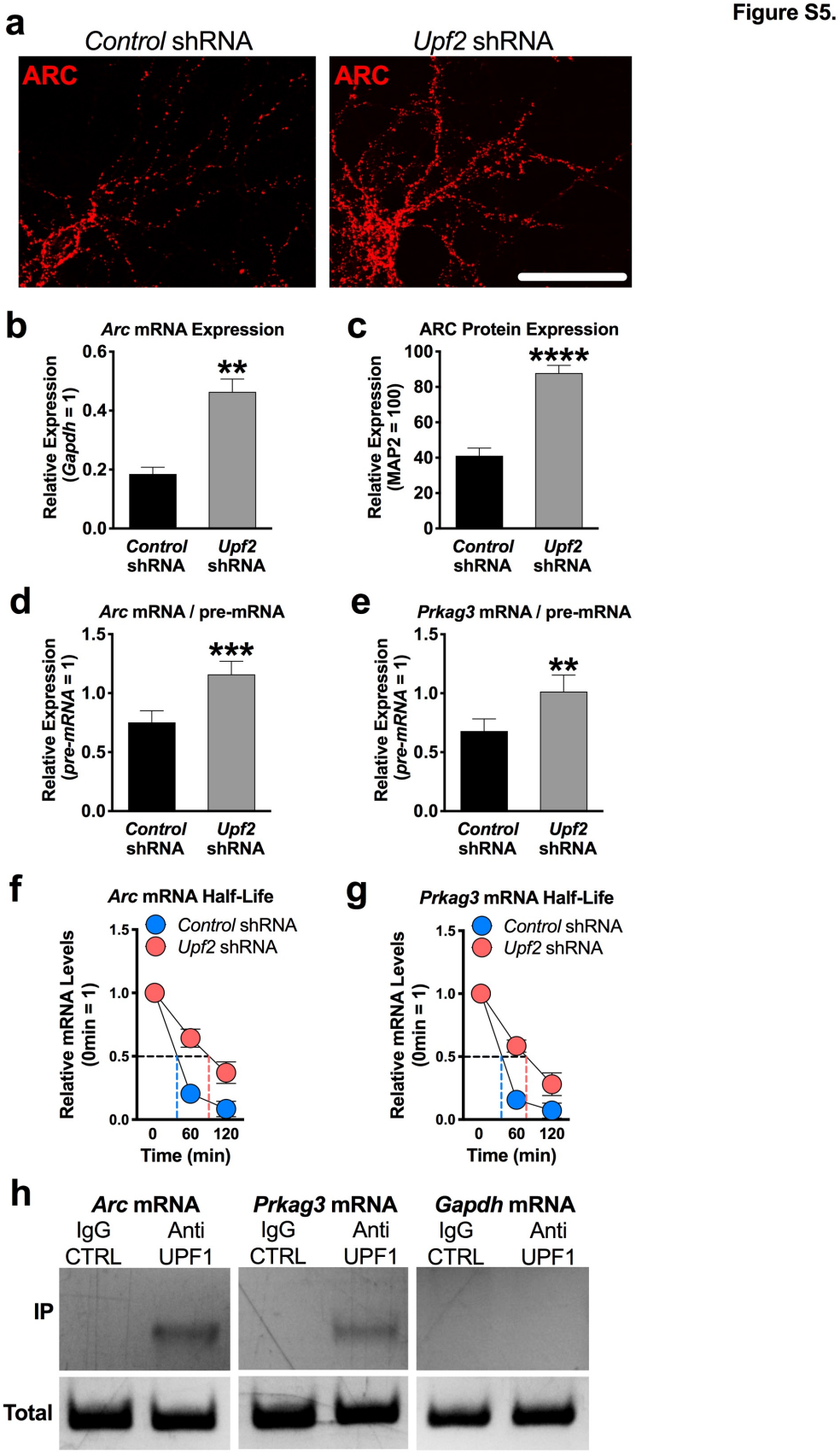
a
Control shRNA
Upf2 shRNA
ARC
ARC
b
Arc mRNA Expression
Relative Expression (Gapdh = 1)
0.6
0.4
0.2
0.0
**
Control shRNA
Upf2 shRNA
c
ARC Protein Expression
Relative Expression (MAP2 = 100)
100
80
60
40
20
0
****
Control shRNA
Upf2 shRNA
d
Arc mRNA / pre-mRNA
Relative Expression (pre-mRNA = 1)
1.5
1.0
0.5
0.0
***
Control shRNA
Upf2 shRNA
e
Prkag3 mRNA / pre-mRNA
Relative Expression (pre-mRNA = 1)
1.5
1.0
0.5
0.0
**
Control shRNA
Upf2 shRNA
f
Arc mRNA Half-Life
Control shRNA
Upf2 shRNA
Relative mRNA Levels (0min = 1)
1.5
1.0
0.5
0.0
0
60
120
Time (min)
g
Prkag3 mRNA Half-Life
Control shRNA
Upf2 shRNA
Relative mRNA Levels (0min = 1)
1.5
1.0
0.5
0.0
0
60
120
Time (min)
h
Arc mRNA
Prkag3 mRNA
Gapdh mRNA
IgG CTRL
Anti UPF1
IgG CTRL
Anti UPF1
IgG CTRL
Anti UPF1
IP
Total

Figure S5. ARC levels are increased upon knockdown of *Upf2* in hippocampal neurons.

a, ARC immunostaining in mouse hippocampal neurons upon knockdown of *Upf2*. Disruption of NMD caused a significant reduction in the total (Figures 1 and S3) and surface (Figure 2) levels of GLUR1 without affecting *GluR1* mRNA levels (Figure 2d). This suggests that NMD regulates GLUR1 surface expression through mechanisms other than transcription or degradation of *GluR1* mRNA. GLUR1 signaling is modulated by the dynamic insertion and removal of GLUR1 receptors at the synaptic surface [14]. The synaptic plasticity protein, ARC, drives the removal of GLUR1 from the surface of synapses. *Arc* mRNA is a known target of NMD. Both *Arc* mRNA and ARC protein are increased upon disruption of NMD [12, 15], suggesting that elevated ARC levels may contribute to the reduced surface expression of GLUR1. To confirm that knockdown of *Upf2* alters endogenous ARC levels, we cultured E16 mouse hippocampal neurons and infected with *control*- or *Upf2*-shRNA lentivirus at DIV7 to disrupt NMD. At DIV21, we performed immunostaining for ARC protein.

b, Quantitative RT-PCR analysis of *Arc* mRNA in UPF2-deficient neurons. *Gapdh* was used as a control transcript. Neurons infected with *Upf2*-shRNA lentivirus displayed exaggerated *Arc* mRNA expression (n=3 biological replicates per group) compared to control neurons.

c, Quantifications of ARC protein in UPF2-deficient neurons. Quantifications of fluorescent intensity, normalized to MAP2, showed that ARC protein levels are also increased in neurons with disrupted UPF2 (per group, n=10 dendrites for analysis of fluorescent intensity). Together, these data confirm that ARC levels are increased upon disruption of *Upf2*. Arc is known to induce internalization of GLUR1 receptor [16]. However, the total levels of GLUR1 are believed to be independent of its internalization rate. While ARC-mediated internalization of GLUR1 influences surface levels, it is presumed not to influence total GLUR1 levels [17] (see also Figure S12). This suggests that while loss of UPF2 does not alter *GluR1* transcription or mRNA degradation (Figure 2d), there is either an increase in GLUR1 protein degradation or a decrease in GLUR1 protein synthesis.

d-h, *Arc* and *Prkag3* mRNAs are natural targets of NMD. To determine whether *Arc* and *Prkag3* are true targets of NMD, we performed a number of experiments including estimated mRNA half-life measurements, mRNA/pre mRNA quantifications, and RNA-immunoprecipitation of targets to the NMD recruitment machinery (namely, UPF1). We quantified relative *Arc* and *Prkag3* mRNAs against pre-mRNA levels in control and UPF2-deficient cells. Both *Arc* (d) and *Prkag3* (e) mRNA levels were increased relative to their pre-mRNA expression upon knockdown of *Upf2*. Subsequently, we also measured estimated, and relative, half-lives of *Arc* and *Prkag3* mRNAs. To do this, we inhibited transcription in control and UPF2-deficient neurons using a final concentration of 10 μg/ml of actinomycin D. The RNA was harvested at 0 min (baseline), 60 min, and 120 min time points and subjected to qRT-PCR. In UPF2-deficient neurons, the estimated half-life of both *Arc* (f) and *Prkag3* (g) mRNAs was increased. This exemplifies that in the absence of UPF2-dependent NMD there is reduced degradation of *Arc* and *Prkag3* mRNAs as would be expected of a natural NMD target. Lastly, to confirm targeting of *Arc* and *Prkag3* mRNAs by the NMD machinery, we co-

immunoprecipitated (see Methods) *Arc* and *Prkag3* mRNAs to UPF1, revealing direct interaction and binding between these physiological mRNAs to the NMD machinery (h). Data are represented as mean ± Standard Error of the Mean (SEM); ** $p < 0.01$, *** $p < 0.001$, **** $p < 0.0001$. Scale bar: 30 μm.

Figure S6.

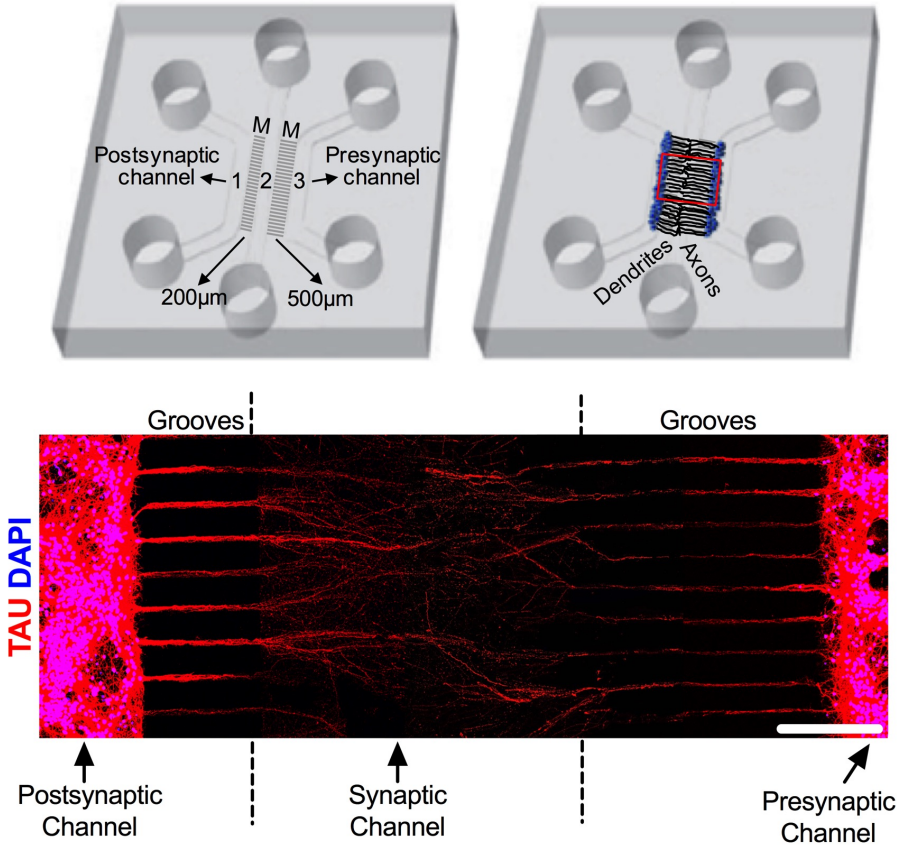
M M
Postsynaptic channel
1 2 3
Presynaptic channel
200µm
500µm
Dendrites
Axons
Grooves
Grooves
TAU DAPI
Postsynaptic Channel
Synaptic Channel
Presynaptic Channel

Figure S6. Axonal penetrance of microgrooves in tripartite microfluidic devices. As shown in the schematic presented here, and the MAP2 immunostaining presented in Figure 3, our custom-engineered tripartite microfluidic device only permits the dendrites of neurons from left channel (channel 1) to penetrate the middle channel, which is referred to as the “synaptic channel” (channel 2). Here, TAU staining shows that axons from both channels extend to the synaptic channel suggesting that axons of both channel 1 and channel 3 can form synapses with dendrites that originated from channel 1. However, due to their limited length, dendrites remain in very close proximity to channel 1 (Figure 3). This tends to restrict dendrite-axon synapses arising from neurons in channel 1 to the proximal-most area of the synaptic channel. Because axons are very long, and the short microgrooves that separate channels 1 and 2 are just 200 μm in length, most channel 1 axons span the entire synaptic channel and go-on to penetrate channel 3. Thus, the majority of the synapses formed in the synaptic channel consist of dendrites projecting from channel 1 and axons originating from channel 3, referred to as the “presynaptic channel”. UPF2 is not expressed in mature axons (Figure S10), and only dendrites from neurons plated in channel 1 can reach the synaptic channel (Figure 3). Therefore, regardless of where the presynaptic axons project from, or where synapses are formed within the synaptic channel, the manipulation of NMD exclusively in channel 1 is confined to postsynaptic dendrites. Scale bar: 200 μm.

Figure S7.

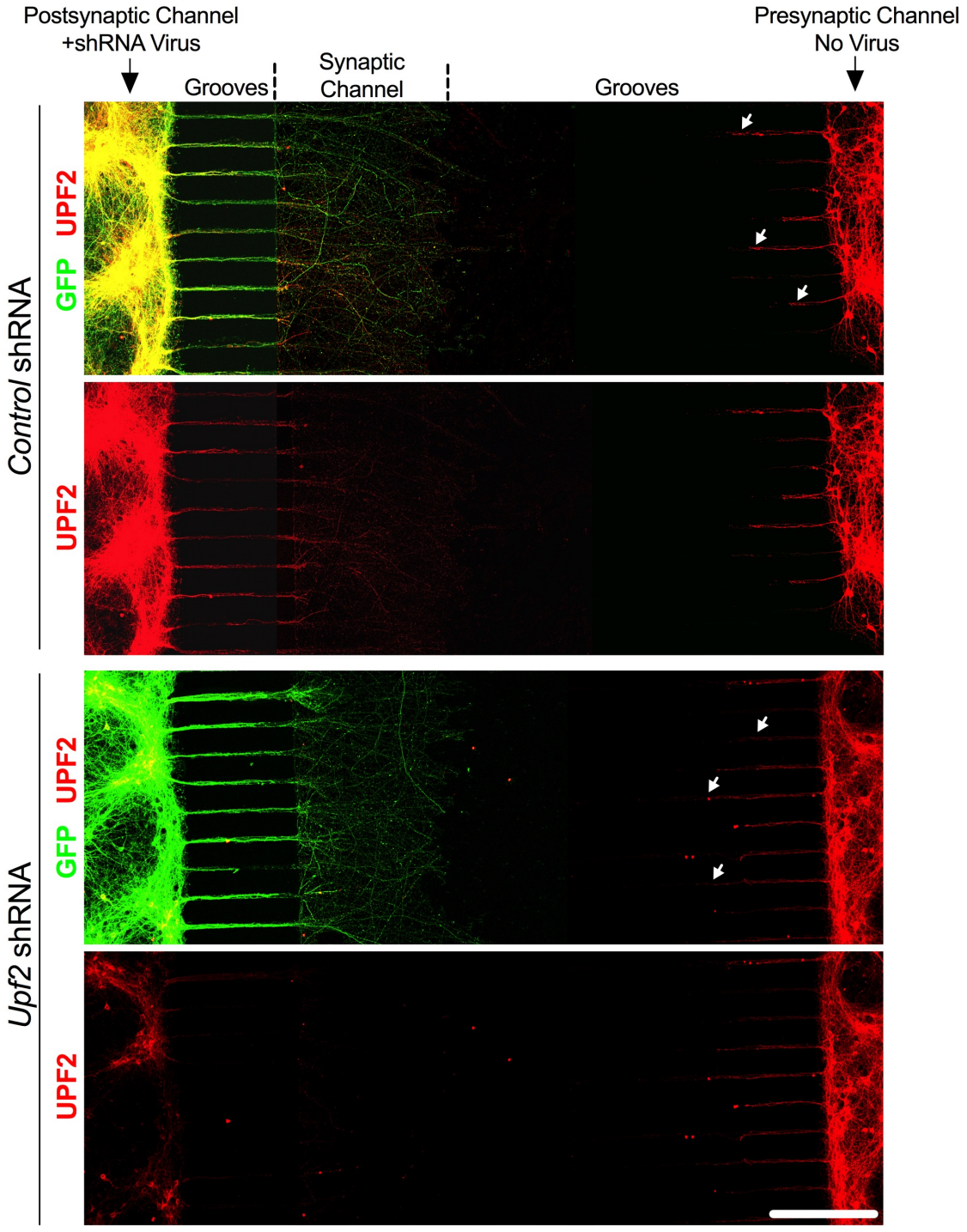
Postsynaptic Channel
+shRNA Virus
Grooves
Synaptic
Channel
Grooves
Presynaptic Channel
No Virus
Control shRNA
GFP UPF2
UPF2
Upf2 shRNA
GFP UPF2
UPF2

Figure S7. Application of *Upf2* shRNA virus exclusively to the postsynaptic channel results in loss of UPF2 in this channel, as well as in dendrites within the synaptic channel, but not in presynaptic channel neurons or their projections. The physical and fluidic isolation of channels is a fundamental feature and component of microfluidic devices, as it permits the selective manipulation/isolation of neuronal populations and compartments. To address the role of NMD in dendrites in synaptic function, we selectively treated postsynaptic channels with *Upf2*-shRNA virus at DIV7. To determine whether the virus application resulted in selective loss of UPF2, we performed immunostainings for UPF2 protein following fixation of cells at DIV13. Consistent with the fluidic isolation of channels, the GFP signal was specific to infected neurons restricted to the postsynaptic channels and their neurites in the synaptic channel. Selective application of the *Upf2*-shRNA virus in the postsynaptic channel resulted in nearly complete loss of UPF2 protein in this channel, as well as in dendrites in the synaptic channel, but not in the presynaptic channel. Because mature axons do not express UPF2 (Figure S10), the UPF2-positive signal in the synaptic channels in the control experiment solely reflects dendritic expression. Consistent with this, dendrites that emerged from the presynaptic channel, which only traveled half way through microgrooves (white arrows), also retained their UPF2 expression in both the *control*- and *Upf2*-shRNA experiments (see Figure 3 and Figure S6 for the comparison of dendrite and axon projection in these grooves). In all experiments that employed *control*- or *Upf2*-shRNAs in tripartite devices, viruses were only applied to the postsynaptic cell body channel of microfluidic devices. Scale bar: 200 μm.

Figure S8.

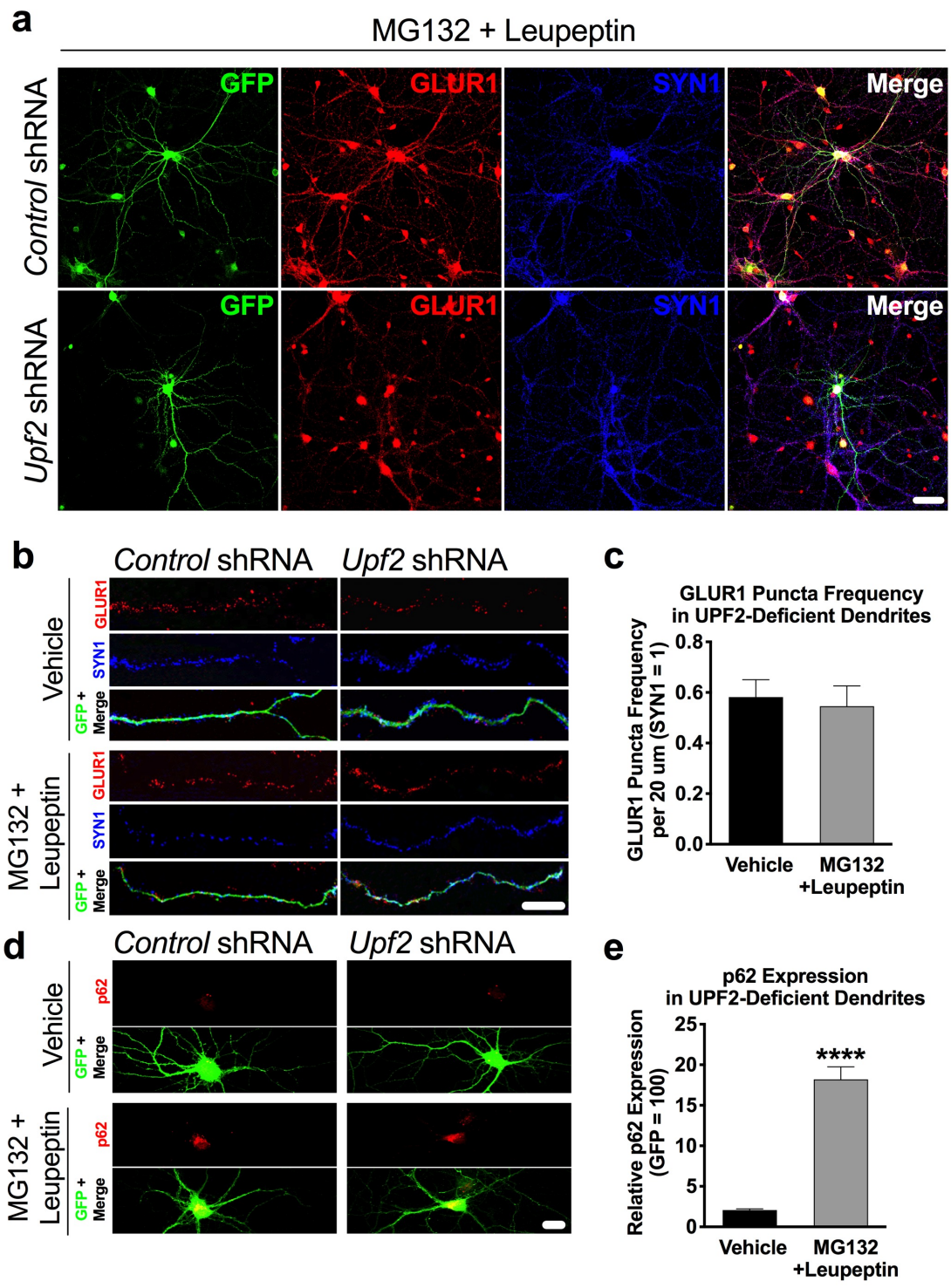
a
MG132 + Leupeptin
Control shRNA
Upf2 shRNA
GFP
GLUR1
SYN1
Merge
b
Control shRNA
Upf2 shRNA
Vehicle
MG132 + Leupeptin
GLUR1
SYN1
GFP + Merge
c
GLUR1 Puncta Frequency in UPF2-Deficient Dendrites
GLUR1 Puncta Frequency per 20 um (SYN1 = 1)
0.0
0.2
0.4
0.6
0.8
Vehicle
MG132 +Leupeptin
d
Control shRNA
Upf2 shRNA
Vehicle
MG132 + Leupeptin
p62
GFP + Merge
e
p62 Expression in UPF2-Deficient Dendrites
Relative p62 Expression (GFP = 100)
0
5
10
15
20
25
****
Vehicle
MG132 +Leupeptin

Figure S8. GLUR1 degradation is not altered upon disruption of UPF2.
Both the surface and total expression of GLUR1 in dendrites is reduced upon knockdown of *Upf2* (Figure S3 and 2). Although the increase in basal internalization rate of GLUR1 (Figure 3a) contributes to the reduction in surface levels of this receptor in the absence of UPF2, it does not explain the decrease in total GLUR1 levels [17]. Since the disruption of NMD does not alter *GluR1* transcription or degradation (Figure 2d), an alteration in the balance of local synthesis and degradation of GLUR1 is likely to account for the overall reduction in the total levels of this receptor upon disruption of NMD. Therefore, we examined the local synthesis of nascent GLUR1 protein (Figure 3) as well as the degradation of GLUR1 protein upon loss of UPF2. Figure 3 shows that the local synthesis of GLUR1 is repressed in UPF2-deficient dendrites. To study GLUR1 protein degradation, we cultured E16 mouse hippocampal neurons in either 24 well plates or in the cell body compartments of tripartite chambers and infected with *Upf2*-shRNA lentivirus at DIV7. In the case of tripartite chambers, we only infected postsynaptic cells with the *Upf2*-shRNA lentivirus. Because endocytosed AMPA receptors can undergo either lysosome- or proteasome-mediated degradation [18-22], we targeted both lysosomal and proteasomal degradation simultaneously. At DIV21, proteasomal and lysosomal degradation were inhibited with 10 μM of the protease inhibitor MG132 and 20 μM of leupeptin, respectively, for 6 hr. For the tripartite experiment, proteasomal and lysosomal degradation were inhibited by treating synaptic channels with 10 μM of the protease inhibitor MG132 and 20 μM of leupeptin, respectively, for 6 hr. To label surface GLUR1, neurons were fixed and stained with an anti-Nterminus-GLUR1 antibody without permeabilization (see also Methods).
a-b, Representative low (regular cultures) and high magnification (in tripartite chambers) images of GLUR1 surface expression in treated and non-treated UPF2-deficient dendrites.
c, Quantification of surface GLUR1 puncta shows that inhibition of proteasomal and lysosomal degradation did not significantly influence GLUR1 puncta frequency in UPF2-deficient dendrites (n=3 biological replicates per group; 11 neurons per group).
d-e, As a positive control, we also measured protein levels of p62 (also know as SQSTM1), which is known to undergo extensive degradation. The levels of p62 were significantly increased following treatment of MG132 and leupeptin in UPF2-deficient dendrites, indicating that protein degradation was successfully inhibited in these experiments.
Data are represented as mean ± SEM. **** $p < 0.0001$. Scale bar: 20 μm.

Figure S9.

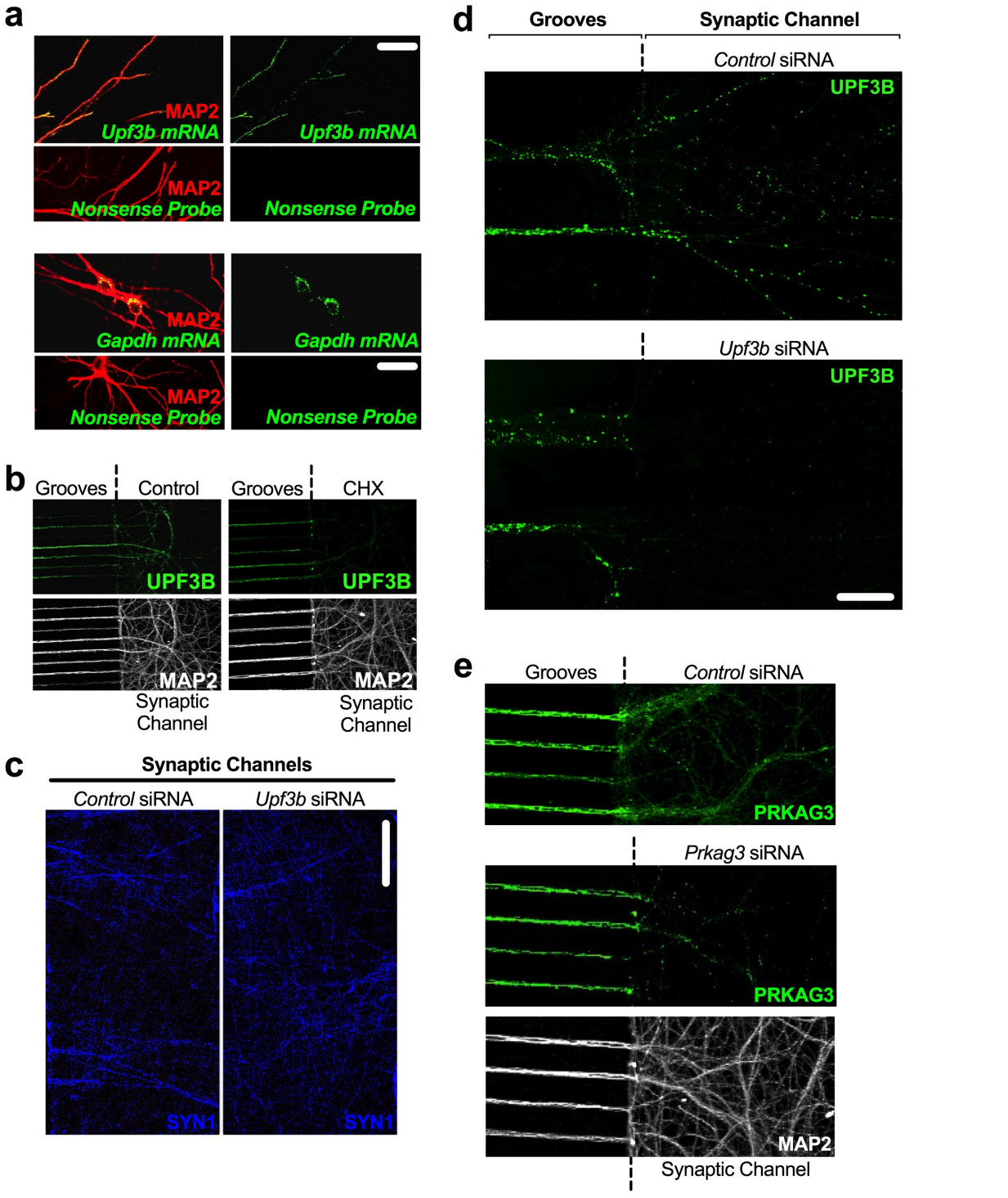
a
MAP2
Upf3b mRNA
Upf3b mRNA
MAP2
Nonsense Probe
Nonsense Probe
MAP2
Gapdh mRNA
Gapdh mRNA
MAP2
Nonsense Probe
Nonsense Probe
b
Grooves
Control
Grooves
CHX
UPF3B
UPF3B
MAP2
MAP2
Synaptic Channel
Synaptic Channel
c
Synaptic Channels
Control siRNA
Upf3b siRNA
SYN1
SYN1
d
Grooves
Synaptic Channel
Control siRNA
UPF3B
Upf3b siRNA
UPF3B
e
Grooves
Control siRNA
PRKAG3
Prkag3 siRNA
PRKAG3
MAP2
Synaptic Channel

Figure S9. UPF3B is locally synthesized in dendrites.
a-b, UPF3B is locally synthesized in hippocampal dendrites. Both dendritic internalization and local synthesis of the GLUR1 receptor are altered upon knockdown of UPF2 (Figure 3). In addition, NMD targets *Arc* and *Prkag3* are subjected to translation-dependent degradation in dendrites (Figure 4). Although these data suggest that NMD might regulate GLUR1 locally in dendrites, there is no direct evidence for the local requirement for NMD in these compartments. To study the specific requirement of locally-occurring NMD in the regulation of GLUR1 within dendrites, we devised a strategy for targeting UPF3B protein (which, like UPF2, is also a specific and major component of the NMD machinery) locally within the synaptic channel of tripartite devices (Figure 4d-e). Previously, analysis of the dendritic transcriptome revealed that *Upf3b* mRNA is trafficked and thereby localized to dendrites [23]. To confirm this, we performed Fluorescent In Situ Hybridization (FISH) on hippocampal neurons with antisense riboprobes against *Upf3b* mRNA at DIV21. Visualization of *Upf3b* FISH revealed punctate labeling (green) along dendrites confirming the localization of *Upf3b* mRNA to these compartments (**a**). *Nonsense* and *Gapdh* probes are shown as additional controls (**a**). Next, we sought to determine if UPF3B is locally synthesized in dendrites. To do this, we inhibited *Upf3b* mRNA translation via dendritic application of Cycloheximide (CHX, 10 μM) and evaluated UPF3B protein in synaptic channels. Specifically, we cultured E16 mouse hippocampal neurons in tripartite chambers and, at DIV21, we treated the synaptic channels with CHX for 6 hr. This resulted in an almost complete loss of UPF3B protein in dendrites (**b**). This suggests that UPF3B is locally synthesized in dendrites. However, we cannot exclude the pleotropic effects of CHX in this experiment given that it blocks all protein synthesis. For instance, it could be that CHX treatment eliminated an unstable protein critical for UPF3B protein stability in dendrites. MAP2 was used to visualize dendrites in both (**a**) and (**b**).
c-d, To determine whether inhibition of local synthesis of UPF3B in synaptic channels alters GLUR1 locally, we selectively treated synaptic channels with siRNAs against *Upf3b* mRNA and evaluated GLUR1 levels (Figure 4d-e). Here, we confirmed that while the treatment of synaptic channels with *Upf3b* siRNA-cocktail (10 nM) for 7 days did not cause an alteration in synaptic potential in these channels (**c**), it led to a complete loss of UPF3B protein (**d**). Note that the expression of UPF3B remained intact within adjacent dendrites in fluidically-isolated microgrooves (**d**).
e, Activated AMPK, which the PRKAG3 subunit contributes to, is known to interrupt translation by either inhibiting the mammalian target of rapamycin (mTOR) kinase or the translation elongation factor 2. These data suggest that NMD might regulate total levels of GLUR1 through degradation of *Prkag3* mRNA in dendrites. To determine whether local PRKAG3 in dendrites modulates GluR1 levels, we inhibited PRKAG3 synthesis in the synaptic channels of tripartite microfluidic devices and examined total GLUR1 levels (Figure 4f). To do this, we targeted *Prkag3* mRNA by systematic application of siRNAs against the *Prkag3* mRNA to synaptic channels. Application of 10 nM of two non-overlapping *Prkag3*-siRNAs to synaptic channels for 7 days, starting at DIV14, led to selective depletion of PRKAG3 within dendrites located in synaptic channels but, once more, not those in microgrooves.
Scale bar: **a** 50 μm, **c** 20 μm, **d** 75 μm.

Figure S10.

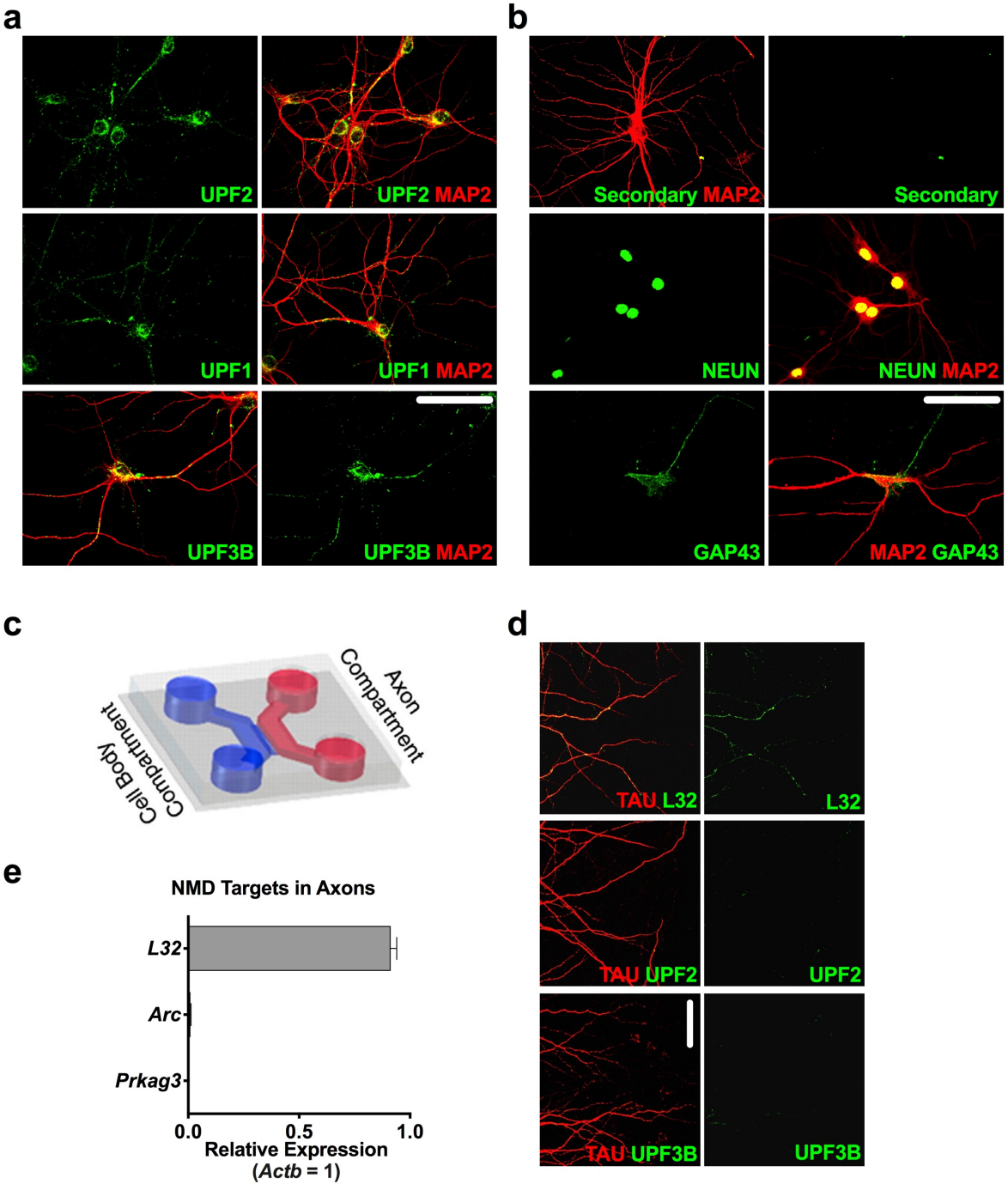
a
UPF2
UPF2 MAP2
UPF1
UPF1 MAP2
UPF3B
UPF3B MAP2
b
Secondary MAP2
Secondary
NEUN
NEUN MAP2
GAP43
MAP2 GAP43
c
Axon Compartment
Cell Body Compartment
d
TAU L32
L32
TAU UPF2
UPF2
TAU UPF3B
UPF3B
e
NMD Targets in Axons
L32
Arc
Prkag3
0.0
0.5
1.0
Relative Expression
(Actb = 1)

Figure S10. Targets of the NMD machinery are not expressed in mature axons.
a-b, Isolated stainings of UPF2, UPF1, and UPF3B in E16 neurons confirms that the major up-frameshift proteins of the NMD machinery are localized to dendrites (MAP2). Immunostainings showing isolated secondary fluorescence without primary, NEUN, and GAP43 are shown as additional controls (**b**) and confirm the specificity of Up-Frameshift proteins within dendrites. While NEUN stained only the nucleus, GAP43 signal is detected in cell bodies and axons but not in dendrites.
c-e, The synaptic channel of tripartite chambers contains both dendrites and axons, raising the possibility that some of the phenotypes observed upon loss of local UPF3B or PRKAG3 in synaptic channels might arise from affected axons. To clarify this, we addressed whether the NMD machinery, as well as *Arc* and *Prkag3* mRNAs*,* are also present in mature axons in addition to dendrites. To do this, we cultured E16 neurons in two-partite microfluidic chambers (scheme adapted from [12]) (**c**). Unlike tripartite chambers used in other experiments, two-partite chambers permit physical isolation of axons [12]. At DIV21, we collected the axonal material and measured the levels of *Arc* and *AMPK* mRNAs by qRT-PCR (**e**). While the axonal mRNA *L32* was readily detected, mature hippocampal axons lacked *Arc* and *Prkag3* mRNAs (n=3 biological replicates). This is consistent with previous reports that the axonal transcriptome shrinks as axons mature [24] and does not include any known NMD targets [25, 26]. Similarly, unlike navigating axons [12], mature axons did not contain the major proteins of the NMD machinery (**d**). These data suggest that the GLUR1 phenotypes observed upon application of siRNAs against both *Upf3b* and *Prkag3* in the synaptic channels of tripartite chambers solely originate from dendrites and not axons. Data are represented as mean ± SEM; Scale bar: **a-b** 50 µm **d** 30 µm.

Figure S11.

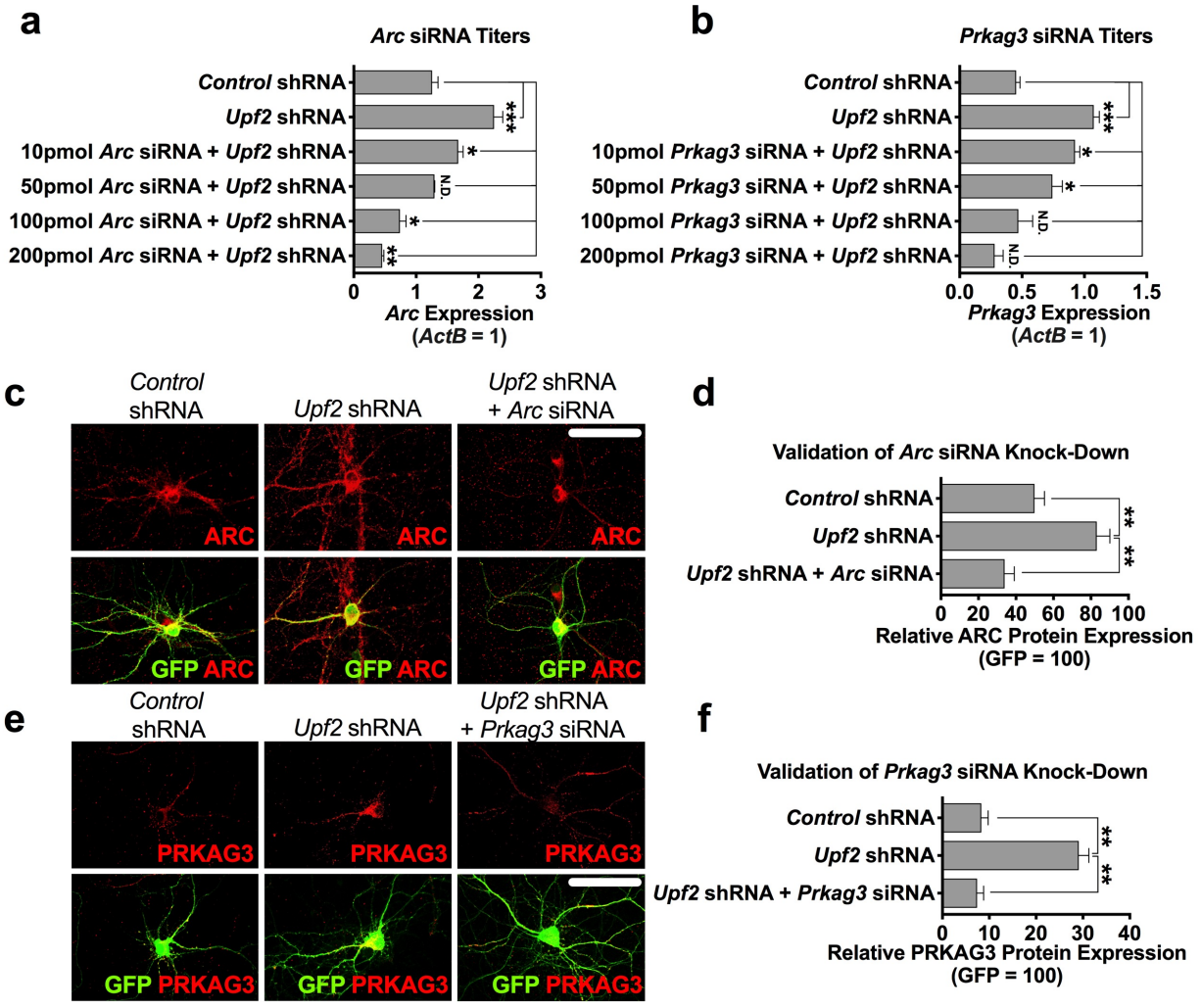
a
Arc siRNA Titers
Control shRNA
Upf2 shRNA
10pmol Arc siRNA + Upf2 shRNA
50pmol Arc siRNA + Upf2 shRNA
100pmol Arc siRNA + Upf2 shRNA
200pmol Arc siRNA + Upf2 shRNA
***
*
N.D.
*
**
0 1 2 3
Arc Expression
(ActB = 1)
b
Prkag3 siRNA Titers
Control shRNA
Upf2 shRNA
10pmol Prkag3 siRNA + Upf2 shRNA
50pmol Prkag3 siRNA + Upf2 shRNA
100pmol Prkag3 siRNA + Upf2 shRNA
200pmol Prkag3 siRNA + Upf2 shRNA
***
*
*
N.D.
N.D.
0.0 0.5 1.0 1.5
Prkag3 Expression
(ActB = 1)
c
Control shRNA
Upf2 shRNA
Upf2 shRNA + Arc siRNA
ARC
GFP ARC
d
Validation of Arc siRNA Knock-Down
Control shRNA
Upf2 shRNA
Upf2 shRNA + Arc siRNA
**
**
0 20 40 60 80 100
Relative ARC Protein Expression
(GFP = 100)
e
Control shRNA
Upf2 shRNA
Upf2 shRNA + Prkag3 siRNA
PRKAG3
GFP PRKAG3
f
Validation of Prkag3 siRNA Knock-Down
Control shRNA
Upf2 shRNA
Upf2 shRNA + Prkag3 siRNA
**
**
0 10 20 30 40
Relative PRKAG3 Protein Expression
(GFP = 100)

Figure S11. *Arc* and *Prkag3* titers for siRNA normalization of exaggerated expression in UPF2-deficient dendrites.

We have identified *Arc* and *Prkag3* as candidate targets in the NMD-mediated regulation of GLUR1 levels within the dendrites and synaptic compartments of hippocampal neurons. We next sought to functionally determine which of these molecules is responsible for depletion of surface GLUR1 in UPF2-deficient dendrites. To do this, we systematically modulated the elevated levels of *Arc* and *Prkag3* in dendrites by siRNA transfection of synaptic channels that contain UPF2-deficient dendrites (Figure 5). First, we applied the *U*pf2-shRNA virus to the postsynaptic-cell channels of tripartite microfluidic devices at DIV7. Starting at DIV14, we treated the synaptic channels of UPF2-deficient dendrites with non-overlapping siRNAs (see Methods) using 10% NeuroPORTER (Sigma).

a-b, As siRNA treatment affects mRNA expression in a concentration-dependent manner [27-30], we first determined the amount of siRNA required to correct the levels of each target in UPF2-deficient dendrites presented in Figure 5. Experiments were completed as descried above, with the exception that synaptic channels were perfused with TRIzol and lysates used for quantitation of *Arc* and *Prkag3* mRNA by qRT-PCR. A panel of *Arc* or *Prkag3* siRNA titers was selectively applied to the synaptic channels of tripartite chambers (n=3 replicates per mRNA and group). In both experiments, and as expected, infection of neurons with *Upf2*-shRNA virus significantly increased the expression of *Arc* (**a**) and *Prkag3* (**b**). Treatment of synaptic channels with *Arc* siRNA cocktail at 10 pmol led to a significant decrease in the expression of *Arc* mRNA in the dendrites of UPF2-deficient postsynaptic neurons, but was still elevated relative to levels observed in the dendrites of postsynaptic neurons in control cultures. Similarly, 100 pmol and 200 pmol titers of *Arc* siRNA cocktail led to a significant downregulation of *Arc* mRNA in the dendrites of UPF2-deficient postsynaptic neurons, but produced expression levels lower than that required to recapitulate the physiological profile of dendritic *Arc* mRNA expression observed in control cultures. However, we observed that 50 pmol of *Arc* siRNA cocktail normalized the expression of *Arc* mRNA in the dendrites of UPF2-deficient postsynaptic neurons, and that these cultures were indistinguishable from control cultures, leading us to adapt this titer in experiments Figure 5. Treatment of the synaptic channels of tripartite chambers with 10 pmol and 50 pmol titers of *Prkag3* siRNA significantly reduced the overexpression of *Prkag3* in the dendrites of UPF2-deficient postsynaptic neurons, but did not restore expression levels to those observed in control cultures. 100 pmol *Prkag3* siRNA titer was chosen for rescue experiments in Figure 5, as raw values closely resembled and statistically did not differ from those observed in the control group (n=3 replicates).

c-f, Next, we sought to validate whether administration of 50 pmol of *Arc* siRNA and 100 pmol *Prkag3* siRNAs to UPF2-deficient dendrites produced ARC and PRKAG3 protein levels similar to controls. To do this, we treated DIV14 hippocampal neurons with either 50 pmol of *Arc* siRNA or 100 pmol *Prkag3 siRNA* for 7 days and stained for the relevant proteins at DIV21. Treatment of UPF2-dendrites with 50 pmol of *Arc* siRNAs resulted in a significant reduction in ARC protein levels (**c-d**) that were comparative and not significantly different from control levels. Similarly, treatment of UPF2-deficient dendrites with 100 pmol *Prkag3* siRNA led to a significant reduction in PRKAG3 protein levels (**e-f**) that were also not significantly different from control levels.

Data are represented as mean ± SEM; * $p < 0.05$, ** $p < 0.01$, *** $p < 0.001$, N.D. indicates “No Difference”. Scale bar: 50 μm.

Figure S12.

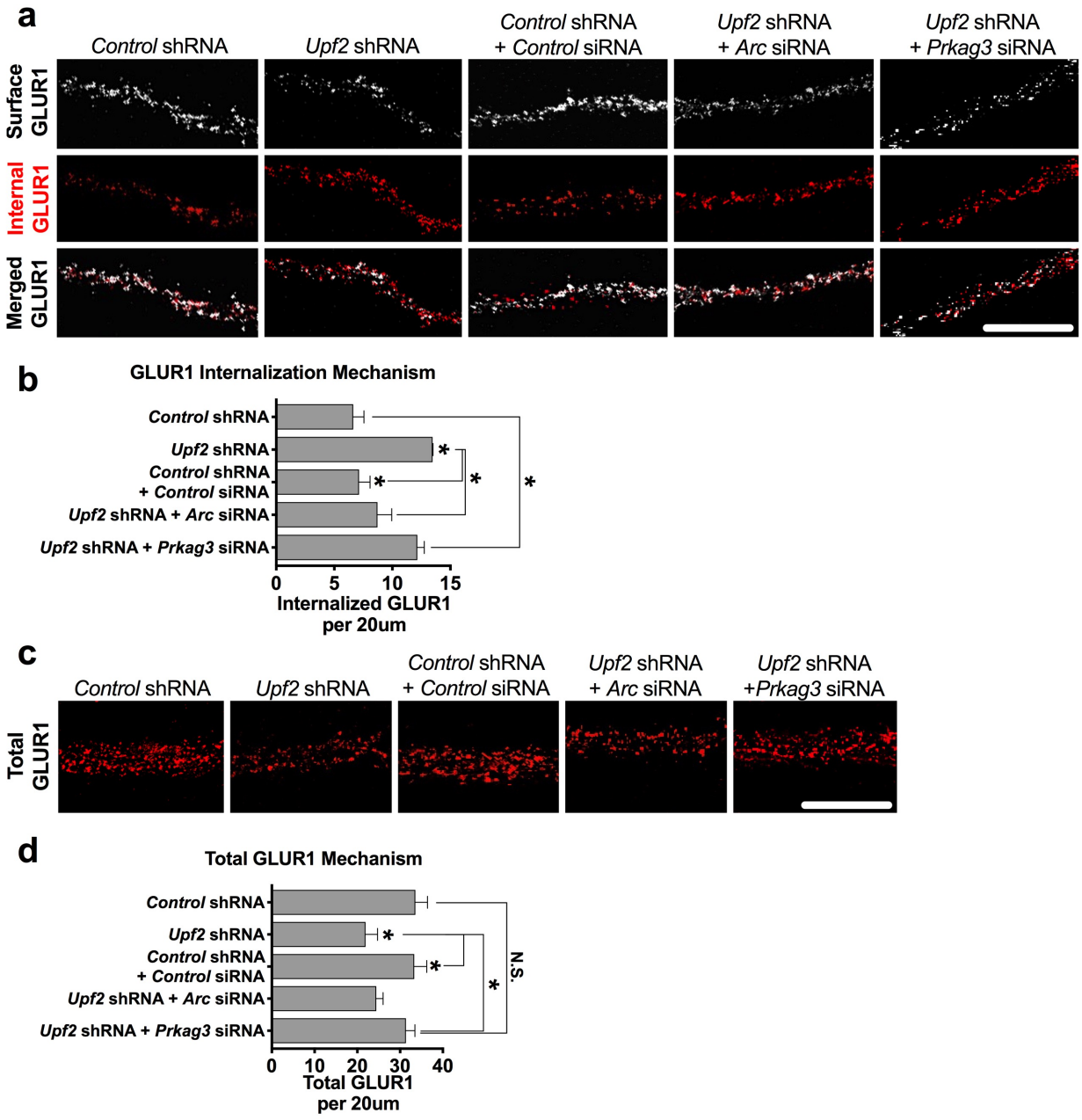
a
Control shRNA
Upf2 shRNA
Control shRNA + Control siRNA
Upf2 shRNA + Arc siRNA
Upf2 shRNA + Prkag3 siRNA
Surface GLUR1
Internal GLUR1
Merged GLUR1
b
GLUR1 Internalization Mechanism
Control shRNA
Upf2 shRNA
Control shRNA + Control siRNA
Upf2 shRNA + Arc siRNA
Upf2 shRNA + Prkag3 siRNA
0 5 10 15
Internalized GLUR1 per 20um
c
Control shRNA
Upf2 shRNA
Control shRNA + Control siRNA
Upf2 shRNA + Arc siRNA
Upf2 shRNA +Prkag3 siRNA
Total GLUR1
d
Total GLUR1 Mechanism
Control shRNA
Upf2 shRNA
Control shRNA + Control siRNA
Upf2 shRNA + Arc siRNA
Upf2 shRNA + Prkag3 siRNA
N.S.
0 10 20 30 40
Total GLUR1 per 20um

Figure S12. Delineating the relative mechanistic contributions of ARC and PRKAG3 to GLUR1 internalization and total GLUR1 expression in dendrites.
Surface levels of GLUR1 were only normalized to levels consistent with controls when both *Arc* and *Prkag3* mRNA levels were modulated in UPF2-deficient dendrites. To delineate the relative mechanism for this effect, we modulated each of these natural NMD targets in UPF2-deficient dendrites but measured basal rates of GLUR1 internalization (**a-b**) and total expression (**c-d**).
a-b, As shown in Figure 3 and described in the Methods, basal rates of GLUR1 internalization were sampled, imaged, and measured in dendrites as previously described. As expected, a significant increase in GLUR1 internalization was detected in UPF2-deficient dendrites at baseline. Application of 50 pmol *Arc* siRNA, but not 100 pmol *Prkag3* siRNA, was sufficient to normalize basal rates of GLUR1 internalization of UPF2-deficient dendrites (n=3 biological replicates per group).
c-d, Similarly, measurements of total GLUR1 levels in dendrites revealed a similar pattern whereby depletion of UPF2 led to a significant decrease in total GLUR1 levels as expected (see Figures 2-3). However, normalization of *Prkag3* mRNA with 100 pmol *Prkag3* siRNA was sufficient to rescue this effect (n=3 biological replicates per group). This result is consistent with our observation of decreased local synthesis of GLUR1 in UPF2-deficient dendrites, and the role of AMPK receptors in inhibiting mTOR-related transcription as discussed previously in this supplementary material and in-text. These experiments identify that the rescue of surface GLUR1 levels in UPF2-deficient dendrites depicted in Figure 5 is specifically achieved via modulation of ARC-induced GLUR1 internalization and PRKAG3-mediated changes in total GLUR1 levels in dendrites.
Data are represented as mean ± SEM; * $p < 0.05$, N.S. indicates “Not Significant”. Scale bar: 30 μm.

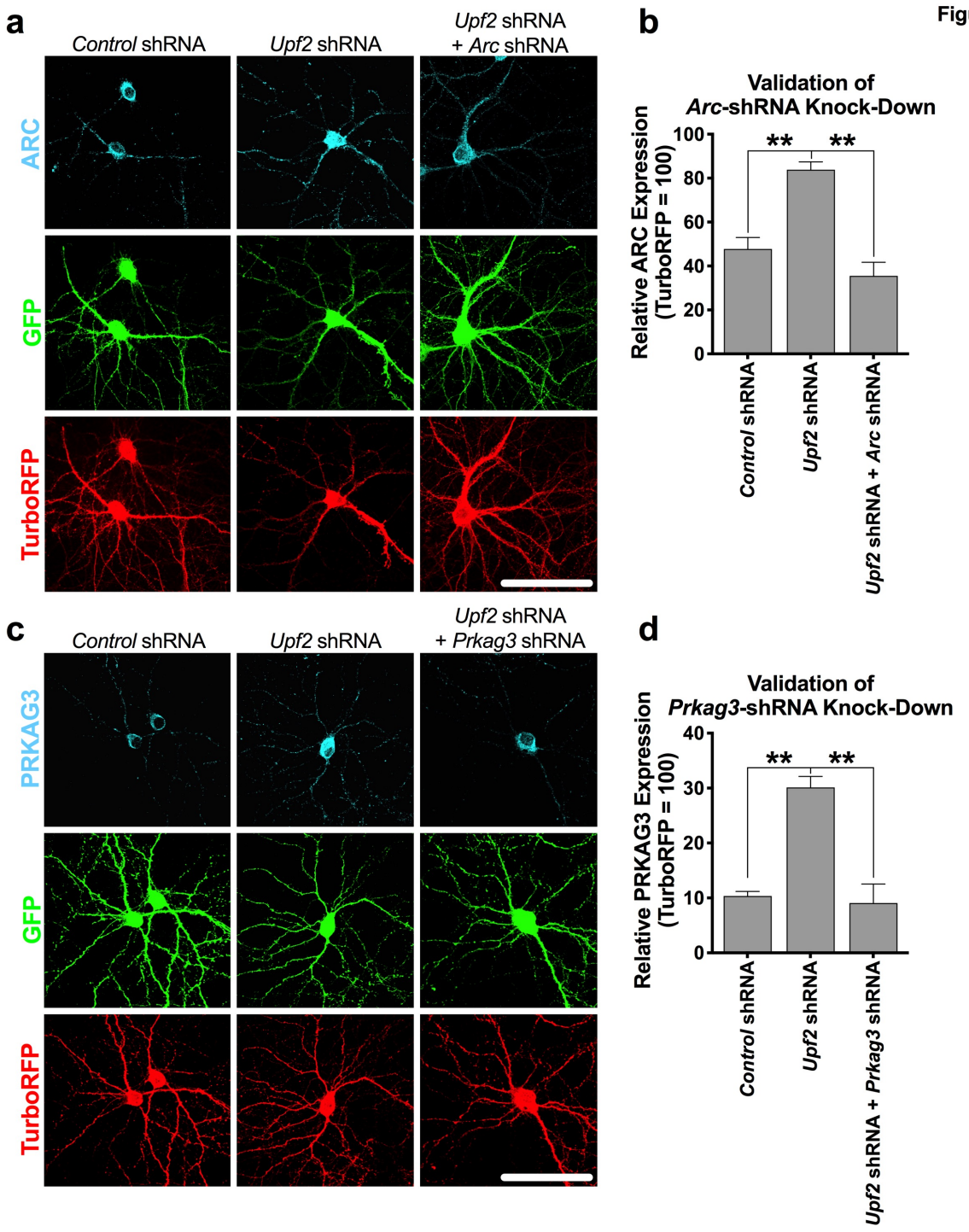
a
Control shRNA
Upf2 shRNA
Upf2 shRNA + Arc shRNA
ARC
GFP
TurboRFP
b
Validation of Arc-shRNA Knock-Down
Relative ARC Expression (TurboRFP = 100)
100
80
60
40
20
0
**
**
Control shRNA
Upf2 shRNA
Upf2 shRNA + Arc shRNA
c
Control shRNA
Upf2 shRNA
Upf2 shRNA + Prkag3 shRNA
PRKAG3
GFP
TurboRFP
d
Validation of Prkag3-shRNA Knock-Down
Relative PRKAG3 Expression (TurboRFP = 100)
40
30
20
10
0
**
**
Control shRNA
Upf2 shRNA
Upf2 shRNA + Prkag3 shRNA

Figure S13.

Figure S13. Validating modulation of ARC and PRKAG3 protein levels by *Arc*-shRNA:TurboRFP and *Prkag3*-shRNA:TurboRFP lentiviruses, respectively.
In Figure 5, we functionally modulate the overexpression of *Arc* and *Prkag3* mRNAs in UPF2-deficient dendrites to establish these NMD targets as the source for reduced surface GLUR1 levels upon depletion of UPF2. We next devised an additional rescue experiment to showcase that this mechanism regulates an *in vivo* phenotype associated with UPF2-depletion, namely hippocampal spine density. To do this, we adapted a viral approach to produce long-lasting downregulation of exaggerated expression of both *Arc* and *Prkag3 in vivo*. To determine whether modulation of ARC and PRKAG3 levels is achieved by *Arc*-shRNA:TurboRFP and *Prkag3*-shRNA:TurboRFP lentiviruses, respectively, we infected DIV14 UPF2-deficient neurons with these viruses and quantified protein expression of each target.
a-b, In neurons infected with *Upf2*-shRNA virus, there was an expected increased in expression of ARC protein. However, in neurons co-infected with *Upf2*-shRNA and *Arc*-shRNA:TurboRFP virus, this overexpression of ARC was diminished to levels consistent with controls (n=3 biological replicates per group).
c-d, Similarly, there was an expected increase in expression of PRKAG3 in UPF2-deficient neurons. However, in neurons co-infected with *Upf2*-shRNA and *Prkag3*-shRNA:TurboRFP virus, the levels of PRKAG3 protein were significantly decreased to levels not significantly different from control neurons (n=3 biological replicates per group). These experiments validate these lentiviral constructs, and their subsequent use, for our *in vivo* rescue experiment (see Figure 5).
Data are represented as mean ± SEM; ** $p < 0.01$. Scale bar: 50 μm.

Figure S14.

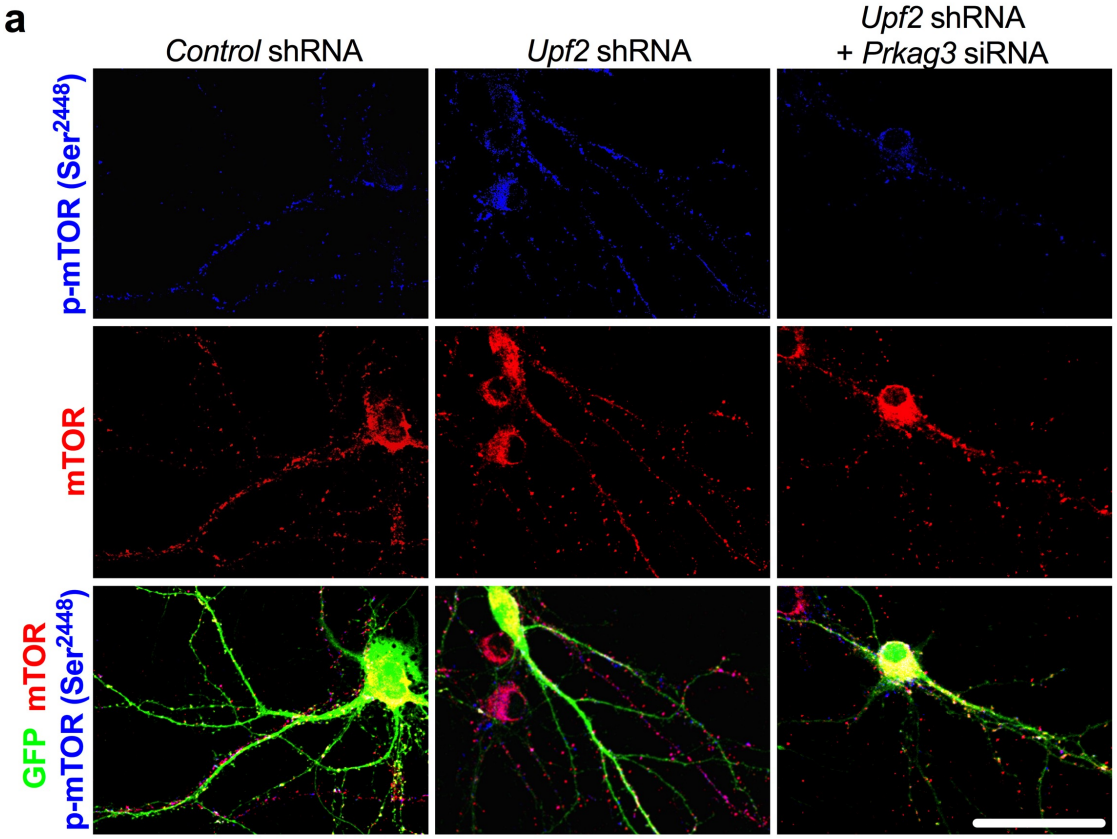
a
Control shRNA
Upf2 shRNA
Upf2 shRNA
+ Prkag3 siRNA
p-mTOR (Ser2448)
mTOR
GFP mTOR
p-mTOR (Ser2448)
b
Regulation of phospho-mTOR in UPF2-Disrupted Cells
Control shRNA
Upf2 shRNA
Upf2 shRNA + Prkag3 siRNA
*
**
N.S.
0
20
40
60
80
Relative phospho-mTOR (Ser2448)
(mTOR = 100)

Figure S14. mTOR pathway as a potential mechanism in AMPK-mediated regulation of total GLUR1 levels.

a-b, As previously discussed, activated AMPK (which PRKAG3 contributes to) has been suggested to interrupt translation via inhibition of the mammalian target of rapamycin (mTOR) kinase [31-36]. Given a decrease in local synthesis of GLUR1 (Figure 3) and that PRKAG3 negatively regulates total GLUR1 levels (Figure 4f), we hypothesized that mTOR activity might be altered in UPF2-deficient neurons and dendrites. To test this, we cultured and infected DIV7 hippocampal neurons with *Upf2*-shRNA virus as previously described, and treated neurons with *Prkag3* siRNA for 7 days starting at DIV14. mTOR phosphorylation can be used as a measure of mTOR activity. At baseline UPF2-deficient neurons exhibited increased mTOR phosphorylation at Ser^{2448}, indicating increased mTOR activity in UPF2-disrupted cells. However, application of 100 pmol of *Prkag3* siRNA for 7 days decreased mTOR phosphorylation to levels not significantly different from controls (n=3 biological replicates per group). These data suggest that PRKAG3 likely influences mTOR activity in cell bodies and dendrites, and this activity could contribute to modulation of GLUR1 synthesis in these compartments. Data are represented as mean ± SEM; * $p < 0.05$, ** $p < 0.01$, N.S. indicates “Not Signifiant”. Scale bar: 50 μm.

Figure S15.

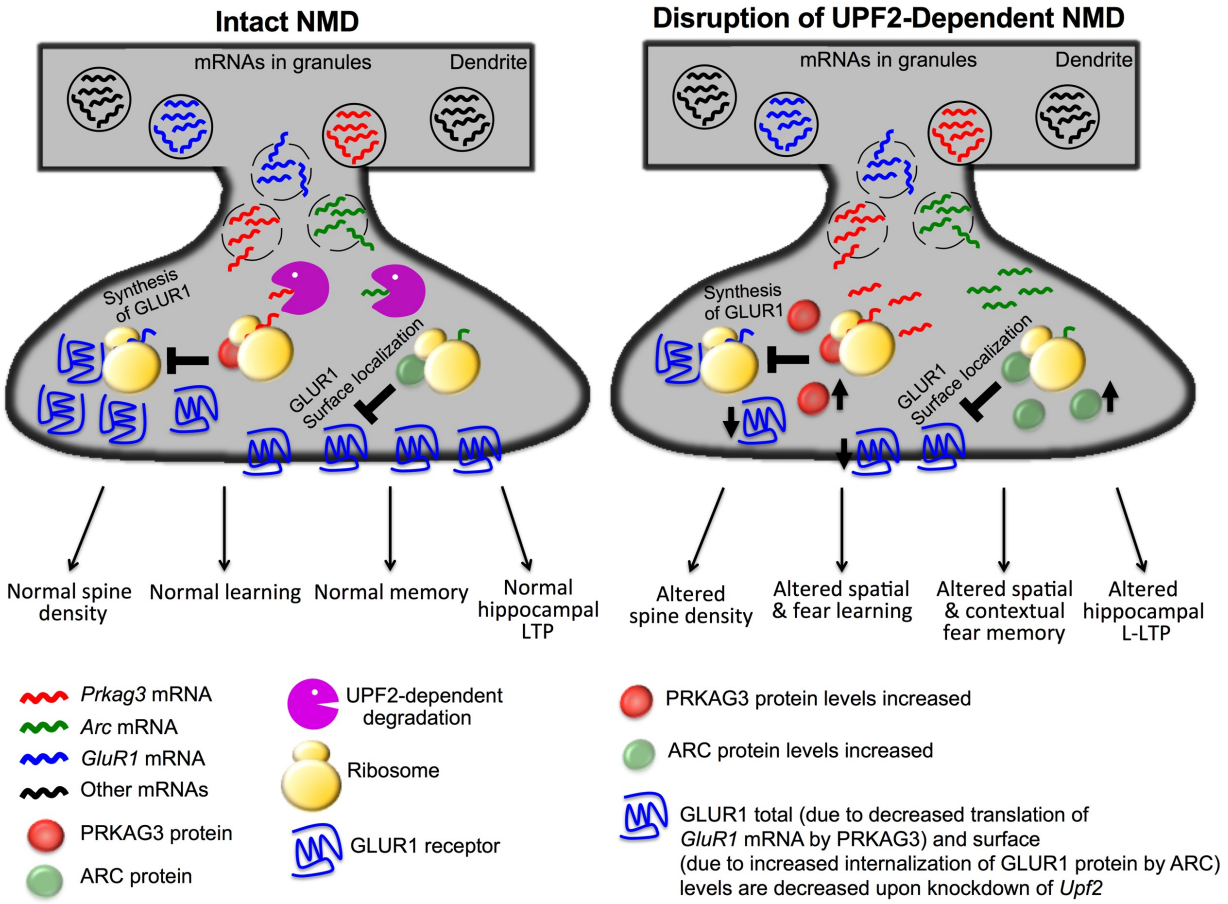
Intact NMD
mRNAs in granules
Dendrite
Synthesis of GLUR1
GLUR1 Surface localization
Normal spine density
Normal learning
Normal memory
Normal hippocampal LTP
Disruption of UPF2-Dependent NMD
mRNAs in granules
Dendrite
Synthesis of GLUR1
GLUR1 Surface localization
Altered spine density
Altered spatial & fear learning
Altered spatial & contextual fear memory
Altered hippocampal L-LTP
Prkag3 mRNA
Arc mRNA
GluR1 mRNA
Other mRNAs
PRKAG3 protein
ARC protein
UPF2-dependent degradation
Ribosome
GLUR1 receptor
PRKAG3 protein levels increased
ARC protein levels increased
GLUR1 total (due to decreased translation of GluR1 mRNA by PRKAG3) and surface (due to increased internalization of GLUR1 protein by ARC) levels are decreased upon knockdown of Upf2

Figure S15. A schematic model for the synaptic regulation of GLUR1 by UPF2-dependent NMD.
We establish that NMD functions in dendrites to modulate local GLUR1 levels, via increased internalization and decreased local synthesis of GLUR1 in dendrites. We mechanistically report that NMD degrades both *Arc* and *Prkag3* mRNAs within dendrites. When NMD is disrupted*, Prkag3* over-accumulates and suppresses local translation of *Glur1* mRNA resulting in decreased nascent GLUR1 protein in dendrites and synapses. Similarly, Arc also over-accumulates and increases GLUR1 internalization rates, which further sequesters surface levels of GLUR1. Therefore, together, the decreased local translation induced by *Prkag3* overexpression and the increased basal internalization of GLUR1 by *Arc* regulates the effect of NMD on surface GLUR1 levels. Co-normalization of both *Arc* and *Prkag3* mRNA levels resulted in the complete recovery of dendritic surface GLUR1 levels in UPF2-deficient dendrites. Together, we mechanistically outlay a role for NMD in plasticity, hippocampus-dependent learning and memory, and the local regulation of GLUR1 specifically in dendrites, establishing that the NMD pathway is not just a passive surveillance pathway but is a critical, activity-dependent, regulator of synaptic function and plasticity.

Supplementary References

1. Weischenfeldt, J., et al., *NMD is essential for hematopoietic stem and progenitor cells and for eliminating by-products of programmed DNA rearrangements.* Genes Dev, 2008. **22**(10): p. 1381-96.
2. Madisen, L., et al., *A robust and high-throughput Cre reporting and characterization system for the whole mouse brain.* Nat Neurosci, 2010. **13**(1): p. 133-40.
3. Kessels, H.W. and R. Malinow, *Synaptic AMPA receptor plasticity and behavior.* Neuron, 2009. **61**(3): p. 340-50.
4. Penzes, P., et al., *Dendritic spine pathology in neuropsychiatric disorders.* Nat Neurosci, 2011. **14**(3): p. 285-93.
5. Addington, A.M., et al., *A novel frameshift mutation in UPF3B identified in brothers affected with childhood onset schizophrenia and autism spectrum disorders.* Mol Psychiatry, 2011. **16**(3): p. 238-9.
6. Laumonnier, F., et al., *Mutations of the UPF3B gene, which encodes a protein widely expressed in neurons, are associated with nonspecific mental retardation with or without autism.* Mol Psychiatry, 2010. **15**(7): p. 767-76.
7. Lynch, S.A., et al., *Broadening the phenotype associated with mutations in UPF3B: two further cases with renal dysplasia and variable developmental delay.* Eur J Med Genet, 2012. **55**(8-9): p. 476-9.
8. Tarpey, P.S., et al., *Mutations in UPF3B, a member of the nonsense-mediated mRNA decay complex, cause syndromic and nonsyndromic mental retardation.* Nat Genet, 2007. **39**(9): p. 1127-33.
9. Nguyen, L.S., et al., *Contribution of copy number variants involving nonsense-mediated mRNA decay pathway genes to neuro-developmental disorders.* Hum Mol Genet, 2013. **22**(9): p. 1816-25.
10. Xu, X., et al., *Exome sequencing identifies UPF3B as the causative gene for a Chinese non-syndrome mental retardation pedigree.* Clin Genet, 2013. **83**(6): p. 560-4.
11. Kim, Y.K., et al., *Mammalian Staufen1 recruits Upf1 to specific mRNA 3' UTRs so as to elicit mRNA decay.* Cell, 2005. **120**(2): p. 195-208.
12. Colak, D., et al., *Regulation of axon guidance by compartmentalized nonsense-mediated mRNA decay.* Cell, 2013. **153**(6): p. 1252-65.
13. Zheng, S., et al., *PSD-95 is post-transcriptionally repressed during early neural development by PTBP1 and PTBP2.* Nat Neurosci, 2012. **15**(3): p. 381-8, S1.
14. Anggono, V. and R.L. Huganir, *Regulation of AMPA receptor trafficking and synaptic plasticity.* Curr Opin Neurobiol, 2012. **22**(3): p. 461-9.
15. Giorgi, C., et al., *The EJC factor eIF4AIII modulates synaptic strength and neuronal protein expression.* Cell, 2007. **130**(1): p. 179-91.
16. Chowdhury, S., et al., *Arc/Arg3. 1 interacts with the endocytic machinery to regulate AMPA receptor trafficking.* Neuron, 2006. **52**(3): p. 445-459.
17. Rial Verde, E.M., et al., *Increased expression of the immediate-early gene arc/arg3.1 reduces AMPA receptor-mediated synaptic transmission.* Neuron, 2006. **52**(3): p. 461-74.

18. Ehlers, M.D., *Reinsertion or degradation of AMPA receptors determined by activity-dependent endocytic sorting.* Neuron, 2000. **28**(2): p. 511-25.
19. Patrick, G.N., et al., *Ubiquitin-mediated proteasome activity is required for agonist-induced endocytosis of GluRs.* Curr Biol, 2003. **13**(23): p. 2073-81.
20. Schwarz, L.A., B.J. Hall, and G.N. Patrick, *Activity-dependent ubiquitination of GluA1 mediates a distinct AMPA receptor endocytosis and sorting pathway.* J Neurosci, 2010. **30**(49): p. 16718-29.
21. Widagdo, J., et al., *Activity-Dependent Ubiquitination of GluA1 and GluA2 Regulates AMPA Receptor Intracellular Sorting and Degradation.* Cell Rep, 2015.
22. Zhang, D., et al., *Na,K-ATPase activity regulates AMPA receptor turnover through proteasome-mediated proteolysis.* J Neurosci, 2009. **29**(14): p. 4498-511.
23. Cajigas, I.J., et al., *The local transcriptome in the synaptic neuropil revealed by deep sequencing and high-resolution imaging.* Neuron, 2012. **74**(3): p. 453-66.
24. Deglincerti, A. and S.R. Jaffrey, *Insights into the roles of local translation from the axonal transcriptome.* Open Biol, 2012. **2**(6): p. 120079.
25. Gumy, L.F., et al., *Transcriptome analysis of embryonic and adult sensory axons reveals changes in mRNA repertoire localization.* RNA, 2011. **17**(1): p. 85-98.
26. Taylor, A.M., et al., *Axonal mRNA in uninjured and regenerating cortical mammalian axons.* J Neurosci, 2009. **29**(15): p. 4697-707.
27. Caffrey, D.R., et al., *siRNA off-target effects can be reduced at concentrations that match their individual potency.* PLoS One, 2011. **6**(7): p. e21503.
28. Elbashir, S.M., et al., *Duplexes of 21-nucleotide RNAs mediate RNA interference in cultured mammalian cells.* Nature, 2001. **411**(6836): p. 494-8.
29. Ki, K.H., et al., *The optimal concentration of siRNA for gene silencing in primary cultured astrocytes and microglial cells of rats.* Korean J Anesthesiol, 2010. **59**(6): p. 403-10.
30. Persengiev, S.P., X. Zhu, and M.R. Green, *Nonspecific, concentration-dependent stimulation and repression of mammalian gene expression by small interfering RNAs (siRNAs).* RNA, 2004. **10**(1): p. 12-8.
31. Gwinn, D.M., et al., *AMPK phosphorylation of raptor mediates a metabolic checkpoint.* Mol Cell, 2008. **30**(2): p. 214-226.
32. Bolster, D.R., et al., *AMP-activated protein kinase suppresses protein synthesis in rat skeletal muscle through down-regulated mammalian target of rapamycin (mTOR) signaling.* J Biol Chem, 2002. **277**(27): p. 23977-23980.
33. Inoki, K., T. Zhu, and K.-L. Guan, *TSC2 mediates cellular energy response to control cell growth and survival.* Cell, 2003. **115**(5): p. 577-590.
34. Horman, S., et al., *Activation of AMP-activated protein kinase leads to the phosphorylation of elongation factor 2 and an inhibition of protein synthesis.* Curr Biol, 2002. **12**(16): p. 1419-1423.
35. Kimura, N., et al., *A possible linkage between AMP-activated protein kinase (AMPK) and mammalian target of rapamycin (mTOR) signalling pathway.* Genes Cells, 2003. **8**(1): p. 65-79.
36. Sarbassov, D.D., S.M. Ali, and D.M. Sabatini, *Growing roles for the mTOR pathway.* Curr Opin Cell Biol, 2005. **17**(6): p. 596-603.